Roles of vacuolar H^+-ATPase in the oxidative stress response of *Candida glabrata*

Hiroshi Nishikawa[1,2], Taiga Miyazaki[1,2,3 *], Hironobu Nakayama[4], Asuka Minematsu[1], Shunsuke Yamauchi[1,5], Kohei Yamashita[1], Takahiro Takazono[1,3], Shintaro Shimamura[1], Shigeki Nakamura[1], Koichi Izumikawa[3], Katsunori Yanagihara[5], Shigeru Kohno[1], Hiroshi Mukae[1,2]

1) Second Department of Internal Medicine, Nagasaki University, Nagasaki, Japan
2) Department of Respiratory Medicine, Unit of Translational Medicine, Nagasaki University Graduate School of Biomedical Sciences, Nagasaki, Japan
3) Division of Infectious Diseases, Department of Molecular Microbiology and Immunology, Nagasaki University Graduate School of Biomedical Sciences, Nagasaki, Japan
4) Faculty of Pharmaceutical Sciences, Suzuka University of Medical Sciences, Mie, Japan
5) Department of Laboratory Medicine, Nagasaki University Graduate School of Biomedical Sciences, Nagasaki, Japan

*Corresponding author

Taiga Miyazaki, MD, PhD

Department of Molecular Microbiology and Immunology, Nagasaki University Graduate School of Biomedical Sciences, 1-7-1 Sakamoto, Nagasaki 852-8501, Japan

Phone: 81-95-819-7273, Fax: 81-95-849-7285, E-mail: taiga-m@nagasaki-u.ac.jp

Running title: Roles of V-ATPase in oxidative stress response

Keywords: *Candida glabrata*, vacuolar H^+-ATPase , catalase, oxidative stress response, superoxide dismutase

Abstract

Vacuolar H^+-ATPase (V-ATPase) is responsible for the acidification of eukaryotic intracellular compartments and plays an important role in oxidative stress response (OSR) but its molecular bases are largely unknown. Here, we investigated how V-ATPase is involved in the OSR by using a strain lacking *VPH2*, which encodes an assembly factor of V-ATPase, in the pathogenic fungus *Candida glabrata*. The loss of Vph2 resulted in increased H_2O_2 sensitivity and intracellular reactive oxygen species (ROS) level independently of mitochondrial functions. The Δ*vph2* mutant also displayed growth defects under alkaline conditions accompanied by the accumulation of intracellular ROS and these phenotypes were recovered in the presence of the ROS scavenger N-acetyl-L-cysteine. Both expression and activity levels of mitochondrial manganese superoxide dismutase (Sod2) and catalase (Cta1) were decreased in the Δ*vph2* mutant. Phenotypic analyses of strains lacking and overexpressing these genes revealed that Sod2 and Cta1 play a predominant role in endogenous and exogenous OSR, respectively. Furthermore, supplementation of copper and iron restored the expression of *SOD2* specifically in the Δ*vph2* mutant, suggesting that the homeostasis of intracellular cupper and iron levels maintained by

V-ATPase was important for the Sod2-mediated OSR. This report demonstrates novel roles of V-ATPase in the OSR in *C. glabrata*.

Introduction

Candida glabrata is an opportunistic fungal pathogen that causes severe invasive infections in immunocompromised patients (Pfaller and Diekema 2007; Trick 2002). In the host environment, phagocytes are the first line of defense against fungal infections. These cells produce reactive oxygen species (ROS) such as superoxide, hydrogen peroxide (H_2O_2), and hydroxyl radicals for damaging biomolecules and killing phagocytosed pathogens (González-Párraga 2003; Thorpe 2004). However, to survive attacks of phagocyte defenses, fungal pathogens synthesize an array of antioxidant enzymes, including superoxide dismutase, catalase, and small antioxidant molecules such as glutathione to eliminate intracellular ROS, and this cellular response is known as the oxidative stress response (OSR) (Anraku 1987; González-Párraga 2003; Lupo 1997; Temple 2005; Thorpe 2004). Inhibition of the OSR of *Candida albicans* has been shown to attenuate its virulence, suggesting that the production of antioxidants is important for virulence (Hwang 2002;

65 Wysong 1998). Thus, understanding OSR mechanisms in pathogenic fungi may be helpful
66 to identify potential targets for the development of new antifungal drugs.

67 The vacuole functions as a primary storage compartment for various ions and
68 solutes, and it regulates cytosolic ion and pH homeostasis (Anraku 1987; Klionsky 1990).
69 Vacuolar H^+-ATPases (V-ATPases) are a family of ATP-dependent proton pumps that are
70 responsible for acidification of intracellular compartments in eukaryotic cells (Bowman BJ
71 and Bowman EJ 1996; Forgac 1998; Stevens and Forgac 1997). Acidification of vacuolar
72 compartments by eukaryotic V-ATPase is essential for several cellular processes, including
73 membrane trafficking (van Weert 1995), lysosomal proteolysis (Creek and Sly 1984),
74 elimination of invading microorganisms in phagosomes (Grinstein 1992), and secondary
75 transport of ions and metabolites (Ohsumi and Anraku 1981; Ohsumi and Anraku 1983;
76 Sze 1985; Tanida 1995).

77 In *Saccharomyces cerevisiae*, V-ATPases are multisubunit enzymes comprising 14
78 subunits organized into two domains: the V_1 domain is a peripheral complex responsible
79 for ATP hydrolysis and the V_0 domain is an integral complex responsible for proton
80 translocation across the membrane (Kane 2006). The genes *VPH2*, *VMA21*, and *VMA22*
81 encode proteins that are not subunits of the final complex but are required for the assembly

of a functional yeast V-ATPase (Graham 1998). Multiple genomic screens have revealed that yeast mutants lacking V-ATPase subunits are sensitive to different forms of exogenous oxidative stress (Higgins 2002; Outten 2005; Thorpe 2004). In addition, yeast V-ATPase subunit (*vma*) mutations lead to increased endogenous oxidative stress, displaying increased ROS levels and protein modifications characteristic of accumulated oxidative damage even in the absence of any exogenous oxidant (Milgrom 2007). However, it is not fully understood how yeast V-ATPase mutation influences this increased sensitivity to exogenous oxidants and endogenous oxidative stress. Furthermore, it has not been reported whether V-ATPase is involved in the OSR of pathogenic fungi. Therefore, in this study, we investigated molecular mechanisms linking V-ATPase and OSR in *Candida glabrata*.

Materials and Methods

Materials

H_2DCFDA was obtained from Invitrogen Corporation (Carlsbad, CA, USA). H_2O_2 solution (30% wt/wt), menadione, NAC, 50% sodium hydroxide solution, ammonium iron sulfate hexahydrate, and copper sulfate pentahydrate were obtained from Wako Pure Chemical Industries Ltd. (Osaka, Japan). Diamide and DEM were obtained from Sigma-Aldrich Co.

(St. Louis, MO, USA). Synthetic complete (SC) medium was prepared as described (Sherman 1991), and the pH was adjusted to 7.2 with 50% sodium hydroxide solution or 0.165M MOPS. The pH of SC medium containing divalent copper and iron ions was adjusted to 7.2 with phosphate-buffered saline to prevent the precipitation of $Cu(OH)_2$ and $Fe(OH)_2$.

Strain and plasmid construction

Gene deletion was performed using a one-step PCR-based technique, as described previously (Gola 2003). Briefly, a 1-kb DNA fragment containing *C. glabrata HIS3* was amplified from pBSK-HIS (Miyazaki 2010b) using primers tagged with 100-bp sequences homologous to the flanking regions of *VPH2*, *CTA1* or *SOD2* ORFs. *C. glabrata* strain KUE200 (Ueno 2007) or 2001HT (Kitada 1995) was transformed with the deletion construct according to a lithium acetate protocol (Cormack and Falkow 1999), and the resulting transformants were selected by histidine prototrophy. For the construction of a Δ*cta1*Δ*sod2* double mutant, a 1-kb DNA fragment containing *C. glabrata TRP1* was amplified from pBSK-TRP (Miyazaki 2013) using primers tagged with 100-bp sequences homologous to the flanking regions of the *SOD2* ORF. The *C. glabrata* Δ*cta1* mutant was

116 transformed with the deletion construct, and the resulting transformants were selected by
117 tryptophan prototrophy. PCR was performed to verify that the desired homologous
118 recombination occurred at the target locus. Reconstitution of the target gene deletion was
119 also performed using a one-step PCR-based technique. A 2.4-kb PCR fragment was
120 amplified from pBSK-5′UTR-VPH2-TRP-3′UTR with the primer pair CgVPH2-F (-849FL)
121 *Bgl*II and CgVPH2-R (+160FL) *Kpn*I. A 3.6-kb PCR fragment was amplified from
122 pBSK-5′UTR-CTA1-TRP-3′UTR with the primer pair CgCTA1-F (-856FL) *Apa*I and
123 CgCTA1-R (+256FL) *Bam*HI. A 2.8-kb PCR fragment was amplified from
124 pBSK-5′UTR-SOD2-TRP-3′UTR with primer pair CgCTA1-F (-875FL) *Apa*I and
125 CgCTA1-R (+234FL) *Bam*HI. The corresponding gene deletion mutant was transformed,
126 and the resulting transformants were selected by tryptophan prototrophy. PCR was
127 performed to verify that the desired homologous recombination occurred at the target locus.
128 For the construction of *CTA1*- and *SOD2*-overexpressing strains, *C. glabrata* strains
129 (2001T and Δ*vph2* mutant) were transformed with pCgACT-CTA1 and pCgACT-SOD2,
130 and the resulting transformants were selected by tryptophan prototrophy.
131 The 2001T and Δ*vph2* mutant strains were converted to *rho0* strains by extended incubation
132 with 25 μg/ml ethidium bromide as described previously (Fox 1991). Two independent

133 *rho0* mutant strains were randomly selected and loss of mitochondrial DNA was confirmed
134 by SYBR Green staining.
135
136 ***Measurement of intracellular ROS levels***
137 The intracellular ROS level in *C. glabrata* was determined by measuring the oxidative
138 conversion of cell-permeable H_2DCFDA to fluorescent dichlorofluorescein (DCF).
139 H_2DCFDA is not fluorescent but can react with ROS to produce the fluorescent derivative
140 DCF. *C. glabrata* cells were incubated with agitation in SC broth (pH 5.0 or 7.2) at 30°C to
141 the logarithmic phase. Cells were washed with distilled water and then diluted to a
142 concentration of 4×10^7 cells/ml of SC broth (pH 5.0 or 7.2). Next, H_2DCFDA was added
143 from a 1 mM stock in ethanol to a final concentration of 10 μM. Cells were incubated at
144 30°C for 15 min. They were washed and resuspended in 200 μl of distilled water.
145 Fluorescence of 200 μl of the sample was measured using a BMG FLUOstar OPTIMA
146 multimode plate reader (BMG Labtech, Offenburg, Germany) with a fluorescence
147 excitation of 485 nm and emission at 530 nm.
148
149 ***Oxidant sensitivity assays***

Oxidant sensitivity assays were performed as described previously (Miyazaki 2010b). Logarithmic-phase cultures of *C. glabrata* cells grown at 30°C in SC broth were adjusted to 2×10^7 cells/ml of the same medium, and then 5 μl of serial 10-fold dilutions were spotted onto SC plates containing H_2O_2, diamide, and menadione at the indicated concentrations. Plates were photographed after 72 h of incubation at 30°C.

Quantitative real-time PCR

Expression levels of some genes encoding antioxidant molecules or enzymes were measured in *C. glabrata* by qRT-PCR. Total RNAs were extracted from logarithmic-phase cells grown in SC broth (pH 5.0 or 7.2) using the RNeasy Mini Kit (Qiagen, Valencia, CA, USA). qRT-PCR was performed as described previously (Izumikawa 2003). One microgram of the extracted RNA was reverse transcribed to cDNA in a final volume of 20 μl using the QuantiTect Reverse Transcription kit (Qiagen), and 3 μl of the resulting cDNA was used as a template of real-time PCR. qRT-PCR was performed using the QuantiTect SYBR Green PCR Kit (Qiagen) and the ABI 7500 Real-Time PCR system (Applied Biosystems) following the manufacturer's instructions. Expression levels of target genes were normalized to 18S rRNA. Results are presented as fold expression relative to the

levels in the wild-type grown in SC broth (pH5.0).

Microarray analysis

Total RNAs were extracted using the RNeasy Mini Kit (Qiagen) from logarithmic-phase *C. glabrata* cells grown in SC broth. The quality of RNA was checked with the RNA 6000 Nano Kit and Agilent 2100 Bioanalyzer. Double-stranded cDNA was synthesized using the Invitrogen SuperScript Double-Stranded cDNA Synthesis Kit and oligo-(dT) primers. The resulting cDNA samples were labeled with Cy3 using the NimbleGen One-Color DNA Labeling Kit and subsequently hybridized to a custom-made 4 × 72 K *C. glabrata* assay (Roche NimbleGen, Tokyo, Japan), wherein each chip measures the expression levels of 5,217 genes from *C. glabrata* CBS138 with six 60-mer probe pairs per gene, with two-fold technical redundancy. The arrays were washed using the NimbleGen Wash Buffer Kit and scanned with a NimbleGen MS 200 Microarray Scanner. Data were quantified using the NimbleScan v2.6 software and normalized as described previously (Irizarry 2003a;,Irizarry 2003b).

Measurement of antioxidant enzyme activity

184 *C. glabrata* cells were grown at 30°C in 50 ml of SC broth (pH 5.0 or 7.2) until the
185 logarithmic phase and then washed with saline. Then, 300 μl of saline was added each
186 sample to be studied. The sample was transferred to a Lysing Matrix tube (MP Biomedicals,
187 Solon, OH, USA) and processed three times in a FastPrep Instrument (MP Biomedicals) for
188 40 s at a setting of 6.0. Next, the cell lysate was centrifuged at 12,000 × *g* for 20 min at 4°C,
189 and the supernatant was removed to prepare the sample solution. Total SOD activity was
190 measured using an SOD Assay Kit-WST following the manufacturer's instructions
191 (Dojindo, Kumamoto, Japan). Mn-SOD activity can be measured by adding potassium
192 cyanide (final concentration: 1 mmol/l) to the sample solution. These reagents inactivate
193 Cu,Zn-SOD and extracellular-SOD activities. Catalase activity was measured using a
194 catalase activity assay kit following the manufacturer's instructions (Biovision, CA, USA).
195 Glutathione was quantified using a GSSG/GSH quantification kit following the
196 manufacturer's instructions (Dojindo, Kumamoto, Japan). The obtained data were for
197 normalized to protein concentration.
198
199 **Results**
200 ***V-ATPase is required for oxidative stress response and cell growth in alkaline***

environment in C. glabrata

To determine whether V-ATPase is involved in the OSR in *C. glabrata*, we measured the sensitivity of a mutant strain lacking *VPH2*, which encodes an assembly factor of V-ATPase, to some oxidative stresses. The *C. glabrata* Δ*vph2* mutant exhibited increased sensitivities to H_2O_2 and diamide compared to the wild-type control, and these sensitivities were reversed in the *VPH2*-reconstituted strain (Fig. 1A). These results suggested that V-ATPase was required for the response to exogenously applied oxidative stress in *C. glabrata*. However, the Δ*vph2* mutant showed similar sensitivity to the superoxide-generating agent menadione as those of the wild-type and *VPH2*-reconstituted strains (Fig. 1A). Cells that are highly sensitive to applied oxidative stress often contain high ROS levels, even in the absence of an exogenous oxidative stress (Moradas-Ferreira *et al*., 1996). To further explore the role of V-ATPase in OSR, we measured the intracellular ROS levels in the wild-type, Δ*vph2* mutant, and *VPH2*-reconstituted strains by using 2′,7′-dichlorofluorescein diacetate (H_2DCFDA). In synthetic complete (SC) medium of pH 5.0, the intracellular ROS level of the Δ*vph2* mutant was approximately 3.0-fold increased compared with that of the wild-type strain, and this was reversed in the *VPH2*-reconstituted strain (Fig. 1B). The growth rate of the Δ*vph2* mutant was slightly lower than that of the

218 wild-type strain at pH 5.0 (Fig. 1C).

219 Next, as alkalization of the medium induces oxidative stress in *S. cerevisiae*
220 (Viladevall 2004), we measured the intracellular ROS level and the growth of these strains
221 in SC medium adjusted to pH 7.2. The intracellular ROS level of the wild-type and the
222 Δ*vph2* mutant at pH 7.2 were approximately 1.6- and 7.3-fold increased compared with that
223 of the wild-type control at pH 5.0, respectively (Fig. 1B). As expected, alkalization of the
224 media induced an increase in intracellular ROS levels of these strains, particularly in the
225 Δ*vph2* mutant. Furthermore, according to the increase in the ROS level, the growth of the
226 Δ*vph2* mutant was suppressed considerably at pH 7.2 compared to that of the wild-type
227 strain (Fig. 1C). Since it seemed that no growth occurred in the Δ*vph2* mutant at pH7.2 for
228 48h, we considered the possibility that the growth after 48h could be attributed to the pH
229 decrease of the media induced by *C. glabrata* cultures. However, the growth curve
230 determined by cell count showed constant growth rate even before 48h and the result was
231 consistent with the growth curve in buffered-media (pH7.2) (Fig. 1D). Based on these
232 results, we considered that the increased OD600 values of the Δ*vph2* mutant culture media
233 at pH7.2 after 48h was not attributed to the pH decrease of the media. These results
234 prompted us to consider the possibility that the increase in intracellular ROS level induced

by alkalization of the media could be the root cause of the impaired growth observed in the Δ*vph2* mutant. Therefore, we examined effects of the ROS scavenger N-acetyl-L-cysteine (NAC) and of the glutathione depletor diethylmaleate (DEM) on the growth and intracellular ROS levels of these strains. The wild-type and Δ*vph2* mutant strains were grown at pH 5.0 or 7.2 in the presence and absence of NAC to the logarithmic phase, and the intracellular ROS levels were measured. The addition of NAC suppressed the increase of intracellular ROS in the Δ*vph2* mutant at pH 7.2 but not at pH5.0 (Fig. 2A). Consistent with this result, the addition of NAC recovered the growth defect of the Δ*vph2* mutant at pH 7.2 in a dose-dependent manner (Fig. 2B). These results suggested that the Δ*vph2* mutant could have defects in an OSR system to deal with high degrees of oxidative stress induced by media alkalization, which could be compensated with NAC.

On the other hand, the addition of 0.5 mM DEM almost completely inhibited the growth of the Δ*vph2* mutant at pH 7.2 (Fig. 2C). Taken together, the results suggest that the growth defect of the Δ*vph2* mutant under alkaline conditions is attributable mainly to its defective OSR.

Mitochondria are not involved in the defective OSR in the Δvph2 mutant

252 Although ROS can arise from a number of different sources and processes, one of the major
253 sources is known to be the mitochondria, and in particular, the electron transport chain
254 (Barros 2004). On the other hand, *rho*^{0} petite mutants lacking mitochondrial DNA have
255 been found to be sensitive to exogenously applied H_2O_2 and menadione, suggesting that the
256 sensitivity is due to a defect in an energy-requiring process needed for detoxification of
257 applied ROS or for repairing oxidative damage (Collinson and Dawes 1992; Grant 2001).
258 To explore the possibility that dysfunctional V-ATPase might induce mitochondrial defects,
259 leading to an impairment of OSR in the Δ*vph2* mutant, we created two independent *rho*^{0}
260 petite mutants in the wild-type and Δ*vph2* backgrounds by ethidium bromide treatment.
261 First, we examined sensitivity of these strains to some oxidative stresses (Fig. 1A). While
262 the wild-type *rho*^{0} petite mutant exhibited slightly higher sensitivity to H_2O_2 than the
263 wild-type strain, the Δ*vph2 rho*^{0} petite mutant exhibited almost the same sensitivity as that
264 of the Δ*vph2* mutant. However, the *rho*^{0} petite mutation did not eliminate the difference of
265 the sensitivity to H_2O_2 between the wild-type strain and the Δ*vph2* mutant, suggesting that
266 mitochondrial defects were not the main source of the defective response to H_2O_2 in the
267 Δ*vph2* mutant.
268 There was no difference of the sensitivity to menadione between the wild-type and Δ*vph2*

269 *rho*^{0} petite mutants as well as between the wild-type and the Δ*vph2* mutant. On the other
270 hand, the high sensitivity of the Δ*vph2* mutant to diamide was partially restored by *rho*^{0}
271 petite mutation. Since diamide is known to rapidly decrease the intracellular glutathione
272 pool, these results suggested that mitochondria could be a source of intracellular ROS and
273 that the Δ*vph2* mutant could have defects in the intracellular OSR system.

274 Next, we measured the intracellular ROS levels in these strains. Petite mutation
275 partially decreased the intracellular ROS levels in both the wild-type and Δ*vph2* mutant
276 strains at pH5.0 and pH7.2 (Fig. 3A). Furthermore, the growth of the Δ*vph2 rho*^{0} petite
277 mutant was partially increased in the media of pH7.2 which induced an increase in the
278 intracellular ROS levels (Fig. 3B). These results were consistent with the reports that a
279 number of different mutants sensitive to oxidative stress demonstrated improved growth in
280 the absence of mitochondrial DNA (Guidot 1993; Haynes 2004). However, petite mutation
281 did not eliminate the difference in the intracellular ROS levels between the wild-type and
282 Δ*vph2* mutant strains, suggesting that mitochondria were not the major source of ROS
283 accumulation and the associated poor growth at alkaline pH in the Δ*vph2* mutant.

284

285 ***The expression levels of CTA1 and SOD2 are dependent on the V-ATPase activity and***

286 ***affect the OSR in C. glabrata***

287 A variety of enzymatic (e.g., superoxide dismutase and catalase) and non-enzymatic (e.g.,
288 glutathione) defense systems are involved in the cellular response to oxidative stresses in
289 yeast, therefore we next considered the possibility that disruption of V-ATPase could affect
290 these oxidative stress defense systems. We conducted genome-wide analyses in the
291 wild-type and Δ*vph2* mutant strains using DNA microarrays and listed the genes involved
292 in the OSR (Table 4). The complete dataset can be found at the NCBI Gene Expression
293 Omnibus (GEO; http//www.ncbi.nlm.nih.gov/geo/) with accession number GSE66984. At
294 pH 5.0, *SOD2* and *CTA1*, which encode a mitochondrial manganese superoxide dismutase
295 and a catalase A, respectively, are downregulated more than 1.5-fold in the Δ*vph2* mutant
296 compared to the wild-type control. At pH 7.4, however, no genes in the Δ*vph2* mutant are
297 downregulated more than 1.5-fold the expression of the wild-type. Next, we compared the
298 expression levels of *SOD2*, *CTA1*, and other well-known genes encoding antioxidants
299 (*SOD1*, *GSH1*, *GSH2*, *GLR1*) by quantitative real-time PCR (qRT-PCR) between the
300 wild-type and Δ*vph2* strains grown at pH 5.0 and 7.2 (Fig. 4A). The expression levels of
301 *CTA1* and *SOD2* in the Δ*vph2* mutant were lower than those in the wild-type strain both at
302 pH 5.0 and pH 7.2. On the other hand, the expression level of *SOD1* in the Δ*vph2* mutant

303 was higher than that in the wild-type strain both at pH 5.0 and pH 7.2. The expression level
304 of the genes in the glutathione pathway did not differ much between the wild-type and the
305 Δ*vph2* mutant at pH 5.0 or pH 7.2. To confirm whether the change in gene expression
306 levels actually reflects the enzyme activity, we performed assays for superoxide dismutase
307 (total SOD and Mn-SOD), catalase activity, and glutathione quantification (Fig. 4B). The
308 activities of Mn-SOD and catalase in the Δ*vph2* mutant were consistently lower than those
309 in the wild-type strain both at pH 5.0 and pH 7.2. On the other hand, total SOD in the
310 Δ*vph2* mutant was higher than that in the wild-type strain. The intracellular glutathione
311 contents were comparable between the wild-type and Δ*vph2* strains. These results
312 suggested that the function of V-ATPase could affect the gene expression and enzyme
313 activities of *CTA1* and *SOD2*.

314 To examine whether the decrease in *CTA1* and *SOD2* expression levels caused the
315 defective OSR in the Δ*vph2* mutant, we created *CTA1*- and *SOD2*-overexpressing strains
316 both in the wild-type and Δ*vph2* mutant backgrounds and measured the gene expression
317 levels by qRT-PCR (Fig. 5A). As the expression levels of these genes were highly
318 increased in the *CTA1*- and *SOD2*-overexpressing strains compared to those in the
319 wild-type and Δ*vph2* mutant, we examined the OSR of these strains. *CTA1* and *SOD2*

320 overexpression in the Δ*vph2* mutant suppressed the increase in intracellular ROS and partly
321 increased cell growth at pH 7.2 but did not induce these effects at pH 5.0 (Fig. 5B and Fig.
322 5C). These results were consistent with the result of NAC addition study. Furthermore, the
323 high sensitivity of the Δ*vph2* mutant to H_2O_2 was restored by *CTA1* overexpression (Fig.
324 5D). However, the sensitivity of the Δ*vph2* mutant to diamide was not restored by *CTA1* or
325 *SOD2* overexpression. These results suggested that the increased intracellular ROS level
326 and the poor growth of the Δ*vph2* mutant at alkaline pH were attributed at least in part to
327 the decreased expressions of *CTA1* and *SOD2*, and the high sensitivity to H_2O_2 was due to
328 the decrease in *CTA1* expression.

329 If these decreases were the root cause of the impaired OSR in the Δ*vph2* mutant,
330 Δ*cta1* and Δ*sod2* mutants are expected to show similar defective phenotypes as the Δ*vph2*
331 mutant. Therefore, we created Δ*cta1* and Δ*sod2* mutants and examined the OSR of these
332 strains. The Δ*cta1* mutant did not show poor growth or an increase in intracellular ROS at
333 pH 5.0 or pH 7.2, unlike the Δ*vph2* mutant (Fig. 6A and Fig. 6B). However, *CTA1*
334 overexpression in the Δ*vph2* mutant suppressed the increase in intracellular ROS level and
335 partly restored the growth at pH 7.2 (Fig. 5B and Fig. 5C). The Δ*cta1* mutant was more
336 sensitive to H_2O_2 than the Δ*vph2* mutant but not sensitive to diamide (Fig. 6C). The

337 sensitivity was reversed in the *CTA1*-reconstituted strain. These results indicated that
338 decreased *CTA1* expression in the Δ*vph2* mutant was the root cause of high sensitivity to
339 H_2O_2 but did not increase intracellular ROS or poor growth at alkaline pH. Conversely, the
340 Δ*sod2* mutant showed an increase in intracellular ROS and poor growth at pH 7.2 but not at
341 pH 5.0, although the extent was less compared to the Δ*vph2* mutant (Fig. 6B and Fig. 6C).
342 These phenotypes were reversed in the *SOD2*-reconstituted strain. The Δ*sod2* mutant was
343 as sensitive to H_2O_2 and diamide as the wild-type (Fig. 6A). Thus, the lowered *SOD2*
344 expression level in the Δ*vph2* mutant could be a part of the cause of the increased
345 intracellular ROS level and poor growth at alkaline pH. We assumed that the
346 downregulation of both *CTA1* and *SOD2* genes in the Δ*vph2* mutant could increase
347 superoxide anion and H_2O_2 levels simultaneously in the cells, leading to the production of
348 reactive hydroxyl radicals, which can induce indiscriminate cellular damage by the
349 Haber–Weiss reaction. We also assumed that the hydroxyl radicals produced in the Δ*vph2*
350 mutant might impair OSR more seriously compared with those of Δ*cta1* and Δ*sod2* single
351 mutants. Therefore, we created a Δ*cta1* Δ*sod2* double mutant and compared the OSR with
352 those of the Δ*vph2*, Δ*cta1*, and Δ*sod2* single mutant strains. The double mutant showed
353 increased intracellular ROS level and poor growth at alkaline pH, but the extent was the

same as in the Δ*sod2* mutant (Fig. 6A and Fig. 6B). Moreover, the double mutant was almost as sensitive to H_2O_2 and diamide as the Δ*cta1* mutant (Fig. 6C). These results suggested that the simultaneous decrease in *CTA1* and *SOD2* expression levels in the Δ*vph2* mutant did not synergistically affect OSR.

Copper and iron are involved in the V-ATPase-dependent SOD2 expression

S. cerevisiae vma mutants are sensitive to several different oxidants and have high intracellular ROS levels even in the absence of an applied oxidant (Milgrom 2007). The yeast vacuole is a significant storage compartment for iron and copper, and specific transport systems of vacuolar iron and copper play an important role in the homeostasis of these metals (Li 2001; Portnoy 2000; Rees 2004). Moreover, copper and iron are limiting factors for the growth of *S. cerevisiae* at alkaline pH, which could lead to oxidative stress (Serrano 2004). Considering these phenomena, we hypothesized that iron and/or copper misregulation in the Δ*vph2* mutant might be a part of the cause of the decrease in *CTA1* and *SOD2* expression, causing defective OSR. First, we performed qRT-PCR to examine *CTA1* and *SOD2* expression levels in the presence and absence of 0.1 mM iron or copper (Fig. 7A). Although addition of iron or copper increased *CTA1* expression level in the Δ*vph2*

371 mutant, similar effects were also observed in the wild-type strain, suggesting that the
372 effects of iron and copper were not related specifically to the decrease of *CTA1* expression
373 in the Δ*vph2* mutant. On the other hand, copper and iron specifically increased *SOD2*
374 expression in the Δ*vph2* mutant but not in the wild-type strain. We confirmed that these
375 metals were involved in the increase of intracellular ROS and the poor growth at alkaline
376 pH, which were caused by the decreased *SOD2* expression in the Δ*vph2* mutant. Addition
377 of 0.1 mM copper suppressed the increase of intracellular ROS level and promoted the
378 growth of the Δ*vph2* mutant at pH 7.2 (Fig. 7B and Fig. 7C). Addition of 0.1 mM iron
379 slightly suppressed the increase of intracellular ROS, but did not promote the growth of the
380 Δ*vph2* mutant at pH 7.2. The effects induced by these metals in the Δ*vph2* mutant were not
381 observed in the wild-type strain.
382
383 **Discussion**
384 In this study, we revealed that deletion of *C. glabrata VPH2*, which encodes the protein
385 required for the assembly of a functional V-ATPase, led to defective response to both
386 endogenous and exogenous oxidative stresses. Mitochondria are intricately linked to the
387 OSR. While mitochondria are needed for energy-requiring process of OSR, they are also

388 the major sources of cellular ROS. In this study, the wild-type *rho*^{0} petite mutant exhibited
389 higher sensitivity to H_2O_2 than the wild-type strain, which was consistent with previous
390 reports with *S. cerevisiae rho*^{0} petite strains (Grant 1997; Jamieson 1992). In the report by
391 Grant *et al*., the sensitivity was restored by the pretreatment with H_2O_2 and menadione at
392 sublethal concentrations, suggesting that respiratory-defective strains are unaffected in their
393 adaptive response to oxidants. Grant *et al*. (Grant 1997) suggested that ATP produced by
394 mitochondria could be required for some energy requiring processes in the OSR including
395 the repair of damaged molecules and the active transport of damaged molecules from the
396 cell and/or into the vacuole for subsequent breakdown reactions. On the other hand, the
397 Δ*vph2 rho*^{0} petite mutant exhibited almost the same sensitivity as that of the Δ*vph2* mutant.
398 These results suggested that the Δ*vph2* mutant was less affected by the above mitochondrial
399 function in resistance to oxidant since the mutant had very low catalase activity, which was
400 required for response to exogenous H_2O_2, independent of mitochondrial function.

401 We revealed that deletion of *C. glabrata VPH2* resulted in decreased expression
402 of *CTA1* and *SOD2*, leading to impaired response to both endogenous and exogenous
403 oxidative stresses (Fig. 8). The high sensitivity of the Δ*vph2* mutant to exogenously applied
404 H_2O_2 was mainly attributed to the decrease in *CTA1* expression (Fig. 5D and Fig. 6C),

405 which was consistent with a previous report that *C. glabrata CTA1* was imperative for
406 resistance to H_2O_2 (Cuéllar-Cruz 2008). On the other hand, the high sensitivity of the
407 Δ*vph2* mutant to H_2O_2 was also partially restored by *SOD2* overexpression. Based on the
408 report that catalase activity was stimulated by H_2O_2 in yeast (Martins 2014), these results
409 reflected that H_2O_2 produced from superoxide anions by *SOD2* overexpression could
410 stimulate the catalase activity. Although the Δ*vph2* mutant also showed high sensitivity to
411 diamide, the sensitivity was not attributed to the decrease in *CTA1* or *SOD2* expression
412 levels. On the other hand, the high sensitivity of the Δ*vph2* mutant was partially restored by
413 rho^0 petite mutation. Since diamide is known to rapidly decrease the intracellular
414 glutathione pool, these results suggested that mitochondria could be a source of
415 intracellular ROS and that the high sensitivity could be ascribed to the decrease in
416 intracellular glutathione content in the Δ*vph2* mutant. On comparing glutathione contents
417 between the wild-type and Δ*vph2* strains, however, no difference was found (Fig. 4B).
418 Consistently, the expression levels of *GSH1* and *GSH2*, both enzymes essential for the
419 production of glutathione in yeast (Grant 2001), were also comparable between the
420 wild-type and Δ*vph2* strains (Fig. 4A). The importance of vacuoles for glutathione
421 sequestration lies in an important defense mechanism for the protection of cells against

422 ROS (Zechmann 2011). On the basis of these findings, the defect in vacuolar distribution of
423 glutathione induced by the deletion of *VPH2* is likely to be attributed to high sensitivity to
424 diamide.

425 The elevated endogenous ROS levels and the accompanied poor growth of the
426 Δ*vph2* mutant at alkaline pH were attributed in part to the decrease in *SOD2* expression
427 (Fig. 5B, Fig. 5C, Fig. 6A and Fig. 6B). The *S. cerevisiae* Δ*sod2* mutant has also been
428 reported to display a significant increase in intracellular ROS level (Doudican 2005). Sod2p
429 specifically localizes to the mitochondrial matrix and mediates the protection of yeast cells
430 against oxygen toxicity in the mitochondria through its enzymatic scavenging of superoxide
431 anion radicals (Gralla and Valentine 1991). Our preliminary results showed that the Δ*vph2*
432 and Δ*sod2* mutants were unable to grow at typical concentrations of nonfermentable carbon
433 sources at alkaline pH. These results suggested that intracellular ROS induced by decreased
434 *SOD2* expression in the Δ*vph2* mutant could cause mitochondrial damage, leading to poor
435 growth at alkaline pH. In contrast, neither mutant showed high sensitivity to the
436 superoxide-generating agent menadione (Fig. 6C). *C. glabrata* has two SOD genes, *SOD1*
437 (Cu,Zn-OD; present in the cytosol and mitochondrial intermembrane space) and *SOD2*
438 (Mn-SOD; localized in the mitochondrial matrix), and the Δ*sod1* mutant is known to be

439 sensitive to menadione (Briones-Martin-Del-Campo 2014). The SOD activity assay in this
440 study revealed that total SOD activity was approximately two orders of magnitude greater
441 than Mn-SOD activity in *C. glabrata* (Fig.4B). Considering that the *SOD1* expression level
442 in the Δ*vph2* mutant was higher than that in the wild-type strain, *SOD1* rather than *SOD2*
443 could be important for resistance to exogenously applied menadione.

444 The OSR in *C. glabrata* is controlled by several well-conserved transcription
445 factors (Cuéllar-Cruz 2008; Roetzer 2010; Roetzer 2011). Yap1 of *C. glabrata*, named
446 Cgap1, is a bZip transcription factor bearing cysteine-rich domains in its N- and C-terminal
447 portions, and it controls the OSR and accumulates transiently in the nucleus during
448 phagocytosis. Skn7 is an oxidative and cell wall stress-responsive transcription factor
449 highly conserved among fungi. A previous genome-wide analysis in *C. glabrata* revealed
450 that one set of genes (*CTA1*, *TRR1/2*, *TSA1/2*, *TRX2*, *GPX2*, and *CCP1*) depended on the
451 presence of both Cgap1 and Skn7 (Briones-Martin-Del-Campo *et al*., 2014). In our
452 genome-wide analysis in the wild-type and Δ*vph2* strains (Table 4), the deletion of *VPH2*
453 decreased *CTA1* expression but conversely increased the expression of *TSA2* and *TRR2*. *C.*
454 *glabrata SOD1* and *SOD2* are expressed constitutively, and their expression levels were
455 found to remain unchanged during peroxide stress in the Δ*cgap1* and Δ*skn7* mutant strains

(Roetzer 2011). On the basis of these results and reports, we consider that V-ATPase regulates *CTA1* and *SOD2* expression levels in parallel with regulation by Cgap1 and Skn7 transcription factors for *C. glabrata* cells to adapt to oxidative stresses.

In the present study, copper specifically increased *SOD2* expression in the Δ*vph2* mutant, leading to the decrease of intracellular ROS level and the increase of growth capacity at alkaline pH. On the other hand, iron slightly increased *SOD2* expression and decreased the intracellular ROS level in the Δ*vph2* mutant, but did not promoted the growth. It has been reported that the availability of copper and iron is a key factor limiting growth of *S. cerevisiae* in alkaline pH (Serrano 2004). In the genome-wide analysis by Serrano *et al*., some genes required for the efficient uptake of these metals were found among the mutations conferring a severe sensitivity to alkaline pH. Consistently, the supplementation with these metal ions and the overexpression of *CTR1* and *FET3*, which encode a high-affinity plasma membrane copper transporter and a low affinity plasma membrane metal cation transporter, respectively, drastically improved growth at alkaline pH. As these metals have a reduced solubility at alkaline pH, these effects suggested that the lowered availability of the metal ions could be improved by the supplementation and the overexpression of the transporters.

S. cerevisiae VMA3 encoding the c subunit of the V_0 sector of V-ATPase is required for normal copper ion homeostasis (Szczypka 1997). In the presence of a sublethal copper ion for all of the vacuolar mutant strains, a Δ*vma3* strain accumulated threefold less copper ions than the wild-type strain. The acidification of vacuoles by V-ATPases is also crucial for proper iron uptake and utilization (Bali 1992; Urbanowski 1999). In a Δ*vma2* strain lacking the b subunit of the V_1 sector of V-ATPase, the loss of the activity could trigger an iron deprivation signal, which might ultimately perturb iron distribution or regulation (Diab and Kane 2013). Mutations in genes essential for vacuole organization and biogenesis have been shown to underlie the alkaline pH-sensitive phenotype (Serrano 2004). Based on these reports, our observation that the Δ*vph2* mutant showed poor growth at alkaline pH and that the growth was promoted by addition of copper could reflect that the Δ*vph2* mutant had low availability of copper at alkaline pH which reduced the solubility since the mutant had defects in the copper transport and regulation.

On the other hand, it was found that a number of genes functionally related to oxidative stress were induced after alkaline stress or were required to display normal sensitivity to alkaline pH (Serrano 2004). Actually, a number of yeast cells exposed to alkaline pH presented fluorescence with dihydrorhodamine 123, suggesting that alkaline

490 pH could lead to oxidative stress. Furthermore, the *vma* mutant contains high ROS levels
491 even in the absence of an applied oxidant (Milgrom 2007). It was reported that
492 supplementation with copper or iron could not improve growth of Δ*lys7* mutant. Lys7 is the
493 copper chaperone that delivers and inserts copper into Sod1 (Culotta 1997). Furthermore,
494 Serrano *et al*. revealed that mutations or deletions in *SOD1*, *SOD2*, and *LYS7* resulted in
495 similar sensitivity to alkaline pH, suggesting the possibility that alkaline stress might lead
496 to oxidative stress and that a certain supply of copper would be necessary to face alkaline
497 pH (Serrano 2004). Based on these reports, we assumed that the decreased sod2 activity in
498 the Δ*vph2* mutant, which seemed to be a partial cause of the increased intracellular ROS
499 and the growth defect at alkaline pH, could be partially ascribed to the impaired uptake or
500 distribution of metal ions. It was demonstrated that supplementation with copper increased
501 the *SOD2* expression level of the Δ*vph2* mutant but not the wild-type strain, thereby
502 suppressing the increase in intracellular ROS level and increasing the growth rate at
503 alkaline pH. These results suggested that copper and iron could be involved in the lowered
504 *SOD2* expression in the Δ*vph2* mutant.

505 To our knowledge, it has been demonstrated for the first time in any yeast
506 including *S. cerevisiae* that V-ATPase plays an important role in the regulation of *CTA1*

and *SOD2* expression level, leading to proper response to endogenous and exogenous oxidative stress. Our results provide new insights into oxidative stress response mechanisms regulated by vacuole, especially V-ATPase, to further understand how fungal pathogens survive the attacks by ROS production of phagocytes. However, as molecular mechanisms linking the vacuolar function and the regulation of *SOD2* and *CTA1* expression remain unclear, future studies are required to determine these molecular mechanisms.

References

Anraku, Y. In *Plant Vacuole*. Marin, B., (ed). New York: Plenum Publishing Corp., 1987, 255–265

Avery, A.M., Avery, S.V. *Saccharomyces cerevisiae* expresses three phospholipid hydroperoxide glutathione peroxidases. *J Biol Chem* 2001; 276: 33730–33735.

Bali, P.K., Aisen, P. Receptor-induced switch in site-site cooperativity during iron release by transferring. *Biochemistry* 1992; 31: 3963–3967.

Barros, M.H., Bandy, B., Tahara, E.B. *et al*. Higher respiratory activity decreases mitochondrial reactive oxygen release and increases life span in *Saccharomyces cerevisiae*.

524 *J Biol Chem* 2004; 279: 49883–49888.

525 Bennett, J.E., Izumikawa, K., Marr, K.A. Mechanism of increased fluconazole resistance in

526 *Candida glabrata* during prophylaxis. *Antimicrob Agents Chemother* 2004; 48: 1773–1777.

527 Bowman, B.J., Bowman, E.J. In *The Mycota III: Biochemistry and Molecular Biology*.

528 Brambl, R., and Marzluf G.A. (eds). Berlin: Springer-Verlag, 1996, 57–83.

529 Briones-Martin-Del-Campo, M., Orta-Zavalza, E., Juarez-Cepeda, J., *et al*. The oxidative

530 stress response of the opportunistic fungal pathogen *Candida glabrata*. *Rev Iberoam Micol*

531 2014; 31: 67–71

532 Collinson, L.P., Dawes, I.W. (1992) Inducibility of the response of yeast cells to peroxide

533 stress. *J Gen Microbiol* 1992; 138: 329–335.

534 Cormack, B.P., Falkow, S. Efficient homologous and illegitimate recombination in the

535 opportunistic yeast pathogen *Candida glabrata*. *Genetics* 1999; 151: 979–987.

536 Creek, K.E., Sly, W.S. *Lysosomes in Biology and Pathology*. Dingle, J.T., and Fell, H.B.

537 (eds). Elsevier Science Publishing Co., Inc., New York, 1984. 63–82.

538 Cuéllar-Cruz, M., Briones-Martin-del-Campo, M., Cañas-Villamar, I., *et al*. High resistance

539 to oxidative stress in the fungal pathogen *Candida glabrata* is mediated by a single catalase,

540 Cta1p, and is controlled by the transcription factors Yap1p Skn7p, Msn2p, and Msn4p.

Eukaryot Cell 2008; **7**: 814–825.

Culotta, V.C., Klomp, L.W., Strain, J., *et al.* The copper chaperone for superoxide dismutase. *J Biol Chem* 1997; 272: 23469–23472.

Diab, H.I., Kane, P.M. Loss of vacuolar H+-ATPase (V-ATPase) activity in yeast generates an iron deprivation signal that is moderated by induction of the peroxiredoxin *TSA2*. *J Biol Chem* 2013; 288: 11366–11377.

Doudican, N.A., Song, B., Shadel, G.S., *et al*. Oxidative DNA damage causes mitochondrial genomic instability in *Saccharomyces cerevisiae. Mol Cell Biol* 2005; 25: 5196–5204.

Dujon, B., Sherman, D., Fischer, G., *et al.* Genome evolution in yeasts. *Nature* 2004; 430: 35–44.

Forgac, M. Structure, function and regulation of the vacuolar (H+)-ATPases. *FEBS Lett* 1998; 440: 258–263.

Fox, T.D., Folley, L.S., Mulero, J.J., *et al*. Analysis and manipulation of yeast mitochondrial genes. *Methods Enzymol* 1991; 194: 149–165.

Gola, S., Martin, R., Walther, A., *et al*. New modules for PCR-based gene targeting in *Candida albicans*: rapid and efficient gene targeting using 100 bp of flanking homology

region. *Yeast* 2003; 20: 1339–1347.

González-Párraga, P., Hernández, J.A., Argüelles, J.C. Role of antioxidant enzymatic defences against oxidative stress H_2O_2 and the acquisition of oxidative tolerance in *Candida albicans. Yeast* 2003; 20: 1161–1169.

Graham, L.A., Hill, K.J., Stevens, T.H. Assembly of the yeast vacuolar H+-ATPase occurs in the endoplasmic reticulum and requires a Vma12p/Vma22p assembly complex. *J Cell Biol* 1998; 142: 39–49.

Gralla, E.B., Valentine, J.S. Null mutants of *Saccharomyces cerevisiae* Cu,Zn superoxide dismutase: characterization and spontaneous mutation rates. *J Bacteriol* 1991; **173**: 5918–5920.

Grant, C.M. Role of the glutathione/glutaredoxin and thioredoxin systems in yeast growth and response to stress conditions. *Mol Microbiol* 2001; 39: 533–541

Grant, C.M., MacIver, F.H., and Dawes, I.W. Mitochondrial function is required for resistance to oxidative stress in the yeast *Saccharomyces cerevisiae. FEBS Lett* 1997; 410: 219–222.

Grinstein, S., Nanda, A., Lukacs, G., *et al*. V-ATPases in phagocytic cells. *J Exp Biol* 1992; 172: 179–192.

575 Guidot, D.M., McCord, J.M., Wright, R.M., *et al*. Absence of electron transport (Rho 0
576 state) restores growth of a manganese-superoxide dismutase-deficient *Saccharomyces*
577 *cerevisiae* in hyperoxia. Evidence for electron transport as a major source of superoxide
578 generation in vivo. *J Biol Chem* 1993; 268: 26699–26703.
579 Haynes, C.M., Titus, E.A., Cooper, A.A. Degradation of misfolded proteins prevents
580 ER-derived oxidative stress and cell death. *Mol Cell* 2004; 15: 767–776.
581 Higgins, V.J., Alic, N., Thorpe, G.W., *et al*. Phenotypic analysis of gene deletant strains for
582 sensitivity to oxidative stress. *Yeast* 2002; 19: 203–214.
583 Hwang, C.S., Rhie, G.E., Oh, J.H., *et al*. Copper- and zinc containing superoxide dismutase
584 (Cu/ZnSOD) is required for the protection of *Candida albicans* against oxidative stresses
585 and the expression of its full virulence. *Microbiology* 2002; 148: 3705–3713.
586 Irizarry, R.A., Bolstad, B.M., Collin, F., *et al*. Summaries of Affymetrix GeneChip probe
587 level data. *Nucleic Acids Res* 2003a; 31: e15.
588 Irizarry, R.A., Hobbs, B., Collin, F., *et al*. Exploration, normalization, and summaries of
589 high density oligonucleotide array probe level data. *Biostatistics* 2003b; 4: 249–264.
590 Izumikawa, K., Kakeya, H., Tsai, H.F., *et al*. Function of *Candida glabrata* ABC
591 transporter gene, PDH1. *Yeast* 2003; 20: 249–261.

592 Jamieson, D.J. *Saccharomyces cerevisiae* has distinct adaptive responses to both hydrogen
593 peroxide and menadione. *J. bacterial* 1992; 174**:** 6678–6681.
594 Kane, P.M. The where, when, and how of organelle acidification by the yeast vacuolar
595 H+-ATPase. *Microbiol Mol Biol Rev.* 2006; 70:177–91.
596 Kitada, K., Yamaguchi, E., Arisawa, M. Cloning of the *Candida glabrata* TRP1 and HIS3
597 genes, and construction of their disruptant strains by sequential integrative transformation.
598 *Gene* 1995; 165: 203–206.
599 Klionsky, D.J., Herman, P.K., Emr, S.D. The fungal vacuole: composition, function, and
600 biogenesis. *Microbiol Rev* 1990; 54: 266–292.
601 Li, L., Chen, O.S., McVey Ward, D., *et al*. CCC1 is a transporter that mediates vacuolar
602 iron storage in yeast. *J Biol Chem* 2001; 276: 29515–29519.
603 Lupo, S., Aranda, C., Miranda-Ham, L., *et al*. Tyrosine is involved in protection from
604 oxidative stress in *Saccharomyces cerevisiae. Can J Microbiol* 1997; 43: 963–970.
605 Martins, D., English, A. M. Catalase activity is stimulated by H_2O_2 in rich culture medium
606 and is required for H_2O_2 resistance and adaptation in yeast. *Redox Biol* 2014; 2: 308–313.
607 Milgrom, E., Diab, H., Middleton, F., *et al*. Loss of vacuolar proton-translocating ATPase
608 activity in yeast results in chronic oxidative stress. *J Biol Chem* 2007; **282**: 7125–7136.

609 Miyazaki, T., Inamine, T., Yamauchi, S., *et al.* Role of the Slt2 mitogen-activated protein
610 kinase pathway in cell wall integrity and virulence in *Candida glabrata*. *FEMS Yeast Res*
611 2010a; 10: 343–352.
612 Miyazaki, T., Nakayama, H., Nagayoshi, Y., *et al*. Dissection of Ire1 functions reveals stress
613 response mechanisms uniquely evolved in *Candida glabrata*. *PLoS Pathog* 2013; 9:
614 e1003160.
615 Miyazaki, T., Yamauchi, S., Inamine, T.. *et al.* Roles of calcineurin and Crz1 in antifungal
616 susceptibility and virulence of *Candida glabrata*. *Antimicrob Agents Chemother* 2010b; 54:
617 1639–1643.
618 Moradas-Ferreira, P., Costa, V., Piper. P., *et al*. The molecular defences against reactive
619 oxygen species in yeast. *Mol Microbiol* 1996; 19: 651–658.
620 Ohsumi, Y., Anraku, Y. Active transport of basic amino acids driven by a proton motive
621 force in vacuolar membrane vesicles of Saccharomyces cerevisiae. *J Biol Chem* 1981; 256:
622 2079–2082.
623 Ohsumi, Y., Anraku, Y. Calcium transport driven by a proton motive force in vacuolar
624 membrane vesicles of *Saccharomyces cerevisiae. J Biol Chem* 1983; 258: 5614–5617.

625 Outten, C.E., Falk, R.L., Culotta, V.C. Cellular factors required for protection from
626 hyperoxia toxicity in *Saccharomyces cerevisiae. Biochem J* 2005; 388: 93–101.
627 Pfaller, M.A., Diekema, D.J. Epidemiology of invasive candidiasis: a persistent public
628 health problem. *Clin Microbiol Rev* 2007; 20: 133–163.
629 Portnoy, M.E., Liu, X.F., Culotta, V.C. *Saccharomyces cerevisiae* expresses three
630 functionally distinct homologues of the nramp family of metal transporters. *Mol Cell Biol*
631 2000; 20: 7893–7902.
632 Rees, E.M., Lee, J., Thiele, D.J. Mobilization of intracellular copper stores by the ctr2
633 vacuolar copper transporter. *J Biol Chem* 2004; 279: 54221–54229.
634 Roetzer, A., Gratz, N., Kovarik, P., *et al*. Autophagy supports *Candida glabrata* survival
635 during phagocytosis. *Cell Microbiol* 2010; 12: 199–216.
636 Roetzer, A., Klopf, E., Gratz, N., *et al.* Regulation of *Candida glabrata* oxidative stress
637 resistance is adapted to host environment. *FEBS Lett* 2011; 585: 319–327.
638 Serrano, R., Bernal, D., Simón, E., *et al*. Copper and iron are the limiting factors for growth
639 of the yeast *Saccharomyces cerevisiae* in an alkaline environment. *J Biol Chem* 2004; 279:
640 19698–19704.
641 Sherman, F. Getting started with yeast. *Methods Enzymol* 1991; 194: 3–21.

642 Stevens, T. H., Forgac, M. Structure, function and regulation of the vacuolar (H+)-ATPase.
643 *Annu Rev Cell Dev Biol* 1997; 13: 779–808.
644 Szczypka, M.S., Zhu, Z., Silar, P., *et al*. *Saccharomyces cerevisiae* mutants altered in
645 vacuole function are defective in copper detoxification and iron-responsive gene
646 transcription. *Yeast* 1997; 3: 1423–1435.
647 Sze, H. H+-translocating Atpases: Advances using membrane vesicles. *Annu Rev Plant*
648 *Physiol* 1985; 36: 175–208.
649 Tanida, I., Hasegawa, A., Iida, H., *et al*. Cooperation of calcineurin and vacuolar
650 H(+)-ATPase in intracellular Ca^{2+} homeostasis of yeast cells. *J Biol Chem* 1995; 270:
651 10113–10119.
652 Temple, M.D., Perrone, G.G., Dawes, I.W. Complex cellular responses to reactive oxygen
653 species. *Trends Cell Biol* 2005; 15: 319–326.
654 Thorpe, G.W., Fong, C.S., Alic, N., *et al*. Cells have distinct mechanisms to maintain
655 protection against different reactive oxygen species: oxidative-stress-response genes. *Proc*
656 *Natl Acad Sci USA* 2004; 101: 6564–6569.

657 Trick, W.E., Fridkin, S.K., Edwards, J.R., *et al*. Secular trend of hospital-acquired
658 candidemia among intensive care unit patients in the United States during 1989–1999. *Clin*
659 *Infect Dis* 2002; 35: 627–630.
660 Ueno, K., Uno, J., Nakayama, H., *et al*. Development of a highly efficient gene targeting
661 system induced by transient repression of *YKU80* expression in *Candida glabrata*.
662 *Eukaryot Cell* 2007; 6: 1239–1247.
663 Urbanowski, J.L., Piper, R.C. The iron transporter Fth1p forms a complex with the Fet5
664 iron oxidase and resides on the vacuolar membrane. *J Biol Chem* 1999; **274**: 38061–38070.
665 van Weert, A.W., Dunn, K.W., Geuze, H.J., *et al*. Transport from late endosomes to
666 lysosomes, but not sorting of integral membrane proteins in endosomes, depends on the
667 vacuolar proton pump. *J Cell Biol* 1995; 130: 821–834.
668 Viladevall, L., Serrano, R., Ruiz, A., *et al*. Characterization of the calcium-mediated
669 response to alkaline stress in *Saccharomyces cerevisiae*. *J Biol Chem* 2004; 279:
670 43614–43624.
671 Wysong, D.R., Christin, L., Sugar, A.M., *et al*. Cloning and sequencing of a *Candida*
672 *albicans* catalase gene and effects of disruption of this gene. *Infect Immun* 1998; 66:
673 1953–1961.

674 Zechmann, B., Liou, L.C., Koffler, B.E., *et al*. Subcellular distribution of glutathione and
675 its dynamic changes under oxidative stress in the yeast *Saccharomyces cerevisiae*. *FEMS*
676 *Yeast Res* 2011; 11: 631–642

TABLE 1 Strains used in this study

Strain	Genotype/description	Reference or source
CBS138	Wild-type	Dujon., 2004
2001T	Δ*trp1* (a derivative of CBS138)	Kitada, 1995
2001HT	Δ*his3*Δ*trp1* (developed from 2001T)	Kitada, 1995
KUE200	Δ*his3*Δ*trp1* Δ*yku80*::*SAT1* flipper (developed from 2001HT)	Ueno, 2007
Δ*vph2*	Δ*vph2*::*HIS3*, Δ*trp1* (developed from KUE200)	This study
Δ*vph2*+*VPH2*	Δvph2::*VPH2-TRP1*, Δ*his3*	This study
Δ*cta1*	Δ*cta1*::*HIS3*, Δ*trp1* (developed from 2001HT)	This study
Δ*cta1*+*CTA1*	Δ*cta1*::*CTA1-TRP1*, Δ*his3*	This study
Δ*sod2*	Δ*sod2*::*HIS3*, Δ*trp1* (developed from 2001HT)	This study
Δ*sod2*+*SOD2*	Δ*sod2*::*SOD2-TRP1*, Δ*his3*	This study
Δ*cta1*Δ*sod2*	Δ*cta1*::*HIS3*, Δ*sod2*::*TRP1* (developed from Δcta1)	This study
2001T+pCgACT-P	2001T containing pCgACT-P	Miyazaki, 2010b
2001T+*CTA1*-OE	2001T containing pCgACT-*CTA1*	This study
2001T+*SOD2*-OE	2001T containing pCgACT-*SOD2*	This study
Δ*vph2*+pCgACT-P	Δ*vph2* containing pCgACT-P	This study
Δ*vph2*+*CTA1*-OE	Δ*vph2* containing pCgACT-*CTA1*	This study
Δ*vph2*+*SOD2*-OE	Δ*vph2* containing pCgACT-*SOD2*	This study

3 **TABLE 2 Primers used in this study**

Primer [a]	**Target**	**Sequence (5′→3′)** [b]
For gene deletion		
CgVPH2 100-F	*VPH2*	*GGCCTTTAAAAAGTGAAAACCTTCCAGAAACTTCCTTCAAG GCGATGAGCTTCAATCTGAGCTGAAGTTCATAGCATATAAA AGCTGTGTTTCCAGTAC***TAATACGACTCACTATAGGGC**
CgVPH2 100-R	*VPH2*	*GGAACAAACAATGAAATTGGTTCATGCATTTGAGTCTAAGG TCCTCGGTCACAACTAAGACATGGTAGCATTAAACAGTCTA GCGACCACCCCATCATA***CGCTCTAGAACTAGTGGATC C**
CgCTA1 100-F	*CTA1*	*CCCTTAAGTCCTTTCTCAATAATCAATAGTTTGGATAGCTATA TAAAGGGTAAGCCTTTACCATCATCAAGCCTTGGAACACAT CCTTTATCCTTTGTT***TAATACGACTCACTATAGGGC**
CgCTA1 100-R	*CTA1*	*CATGAACATTAGTGTCACATTTCTTGTTCCCATATTAAATAAA TACCCACCTAATACCGGTTAGTTGAGATGAGAAAAGCTAGC GCTTTGAACTGAACT***CGCTCTAGAACTAGTGGATCC**
CgSOD2 100-F	*SOD2*	*CAATCCAGGGCTACCTTGCACAATACATATATATATAGAGGA TAATTACTCATCATGTACACGGACGTTCACCGAAAGTACAAC ATCTAACTTGACTTT***TAATACGACTCACTATAGGGC**
CgSOD2 100-R	*SOD2*	*CCGTGTCGATGCTGCCCTTCCCAGGTTGTAGTCTATTTTAA GTGTTAAATTTATTTTAAGTATAGTGCTTACTTTAGGTGCGAA TATGTAGAGAGAGTT***CGCTCTAGAACTAGTGGATCC**

For gene reconstitution		
CgVPH2-F (-849FL) *Bgl*II	*VPH2*	CTAGATCTTCACCGCCTAAACCG
CgVPH2-R (+41FL) *Xho*I	*VPH2*	CCGCTCGAGCAAGCAGGCTGATAACACAGGG
CgVPH2-F (+1FL) *Kpn*I	*VPH2*	AAGGTACCCCAAAGTAATGTTGTCTGCCCCT
CgVPH2-R (+160FL) *Kpn*I	*VPH2*	AAGGTACCGACATGGTAGCATTAAACAGTCTAGCG
CgCTA1-F (-856FL) *Apa*I	*CTA1*	TATGGGCCCTCTCACCAACAAAATGCTGCC
CgCTA1-R (+1FL) *Apa*I	*CTA1*	TATGGGCCCTACGTGGTTCAAAAGCGCAC
CgCTA1-F (+1FL) *Bam*HI	*CTA1*	CGCGGATCCGTGCGCTTTTGAACCACGTA
CgCTA1-R (+256FL) *Bam*HI	*CTA1*	CGCGGATCCGACATAACATCAAGTCCCAAACC
CgSOD2-F (-875FL) *Apa*I	*SOD2*	TATGGGCCCCTAAACCCCCTCCATCGCTTAC
CgSOD2-R (+19FL) *Apa*I	*SOD2*	TATGGGCCCGGTGCGAATATGTAGAGAGAGTTG
CgSOD2-F (+19FL) *Bam*HI	*SOD2*	CGCGGATCCCAACTCTCTCTACATATTCGCACC
CgSOD2-R (+234FL) *Bam*HI	*SOD2*	CGCGGATCCTTGTAATGGTCGGTGTTAAGCG
For gene overexpression		
CgCTA1-F1-*Bam*	*CTA1*	CGGGATCCATGTCCGCTAATCCAACTAACACTTCC
CgCTA1-R508FL-*Xho*	*CTA1*	CCGCTCGAGTATGTTGGACTACGACGGTCTCGC
CgSOD2-F1-*Bam*	*SOD2*	CGGGATCCATGTTGTCTACGTCTAGGATTGCTTTC
CgSOD2-R711-*Xho*	*SOD2*	CCGCTCGAGCTATTTAGTGACTTTGGATGTTTCGTACCT
For qRT-PCR		
CgCTA1-F317	*CTA1*	TCGGTGGTGAAAAGGGTTCTG
CgCTA1-R473	*CTA1*	TGGGTGTGGATGAAATGTGGG
CgSOD1-F133	*SOD1*	GGTTTCCACATCCACGAGTTCG

CgSOD1-R262	*SOD1*	TGTTTCCCAAGTCACCGACG
CgSOD2-F154	*SOD2*	TCCAAGCACCACCAGACCTATG
CgSOD2-R367	*SOD2*	CTTCACCACCACCGTTCTTCTC
CgGSH1-F1094	*GSH1*	TGGGAGGGAACGAAAACAAGTC
CgGSH1-R1266	*GSH1*	CTCTTCAAAAGTGGAAATCGGGTC
CgGSH2-F1098	*GSH2*	TGAACCTCATCGTTTTGTGCTG
CgGSH2-R1369	*GSH2*	GCCATCCGGCTGTTTCTGTTG
CgGLR1-F1262	*GLR1*	GTGAAGGTCCAAATGAGAAGGTTG
CgGLR1-R1388	*GLR1*	GCCACACAGTTGTCAAAATCAGC
CgCTA1-F317	*CTA1*	TCGGTGGTGAAAAGGGTTCTG
CgCTA1-R473	*CTA1*	TGGGTGTGGATGAAATGTGGG
CgSOD1-F133	*SOD1*	GGTTTCCACATCCACGAGTTCG
CgSOD1-R262	*SOD1*	TGTTTCCCAAGTCACCGACG
CgSOD2-F154	*SOD2*	TCCAAGCACCACCAGACCTATG
Cg18S-F	18S rRNA	TGACTCAACACGGGGAAACTCAC
Cg18S-R	18S rRNA	CACTCCACCAACTAAGAACGGC

[a] "Cg" stand for *Candida glabrata*. "F" and "R" indicate forward and reverse primers, respectively.

[b] Sequences homologous to flanking regions of the target ORF are shown in italics.

Sequences shown in boldface are present in pBSK-HIS and pBSK-TRP. Restriction sites

are underlined.

9 **TABLE 3 Plasmids used in this study**

Plasmid	Description	Reference
pBSK-HIS	pBluescript II SK+ (Stratagene, La Jolla, CA) containing *C. glabrata HIS3* at the *Xho*I site	Miyazaki et al., 2010b
pBSK-TRP	A 1-kb *Xho*I fragment containing *C. glabrata TRP1* was excised from pCgACT and inserted into the *Xho*I site of pBluescript II SK+ (Stratagene).	Miyazaki et al., 2013
pBSK-5′UTR-VPH2-TRP-3′UTR	A 1.5-kb *Bam*HI-*Sal*I PCR fragment containing the 5′UTR and ORF of *C. glabrata VPH2* was inserted into the *Bam*HI-*Sal*I site of pBSK-TRP, and then a 160-bp *Kpn*I PCR fragment containing the 3′UTR was inserted into the *Kpn*I site of pBSK-5′UTR-VPH2-TRP.	This study
pBSK-5′UTR-CTA1-TRP-3′UTR	A 2.4-kb *Apa*I PCR fragment containing the 5′UTR and ORF, and a 250-bp *Bam*HI PCR fragment containing the 3′UTR of *C. glabrata CTA1* were inserted into the *Apa*I and *Bam*HI sites of pBSK-TRP, respectively.	This study
pBSK-5′UTR-SOD2-TRP-3′UTR	A 1.6-kb *Apa*I PCR fragment containing the 5′UTR and ORF, and a 250-bp *Bam*HI PCR fragment containing the 3′UTR of *C. glabrata SOD2* were inserted into the *Apa*I and *Bam*HI sites of pBSK-TRP, respectively.	This study
pCgACT-P	A 1-kb *Sac*I-*Kpn*I fragment containing the *S. cerevisiae PGK1* promoter, polylinker, and *C. glabrata HIS3* 3′UTR was excised	Miyazaki et al., 2010b

	from pGRB2.2 and inserted into the *Sac*I-*Kpn*I site of pCgACT	
pCgACT-CTA1	A 2.0-kb *Bam*HI-*Xho*I PCR fragment containing *C. glabrata CTA1* was inserted into the *Bam*HI-*Xho*I site of pCgACT-P	This study
pCgACT-SOD2	A 0.7-kb *Bam*HI-*Xho*I PCR fragment containing *C. glabrata SOD2* was inserted into the *Bam*HI-*Xho*I site of pCgACT-P	This study

TABLE 4 Expression levels of genes involved in oxidative stress response in *Candida glabrata* wild-type and Δ*vph2* mutant strains

	vph2/WT						Sc_ortholog [a]	Description (Sc) [b]
	pH 5.0			pH 7.4				
	1	2	average	1	2	average		
CAGL0E04356g	-1.86	-1.35	-1.56	-1.19	-1.05	-1.12	*SOD2*	Ortholog(s) have superoxide dismutase activity
CAGL0K10868g	-1.57	-1.57	-1.57	-1.40	-1.32	-1.36	*CTA1*	Putative catalase A; gene is downregulated in azole-resistant strain and regulated by oxidative stress and glucose starvation; protein abundance increased in ace2 mutant cells
CAGL0J11484g	-1.38	-1.57	-1.47	-1.41	-1.00	-1.17	*DUG3*	Component of the Dug1p-Dug2p-Dug3p complex involved in glutathione degradation; required for glutathione utilization in *C. glabrata* when glutathione import is enabled by the expression of the *S. cerevisiae* Opt1p transporter
CAGL0G02101g	-1.51	-1.39	-1.45	1.03	1.21	1.12	*ECM4*	Putative omega class glutathione transferase; gene is downregulated in the azole-resistant strain
CAGL0K00231g	-1.43	-1.43	-1.43	-1.30	-1.11	-1.20	*OXP1*	Ortholog(s) have 5-oxoprolinase (ATP-hydrolyzing) activity and play a role in glutathione metabolic process and cytosol localization
CAGL0L03630g	-1.28	-1.33	-1.30	-1.22	-1.28	-1.25	*GSH1*	Putative gamma glutamylcysteine synthetase, essential for viability
CAGL0C01705g	-1.31	-1.27	-1.29	1.03	1.01	1.02	*GPX2*	Putative glutathione peroxidase
CAGL0H05665g	-1.35	-1.19	-1.26	-1.25	-1.15	-1.20	*GLR1*	Predicted glutathione oxidoreductase involved in oxidative stress response

CAGL0C03850g	-1.17	-1.19	-1.18	1.00	-1.15	-1.07	*DOT5*	Ortholog(s) have thioredoxin peroxidase activity, role in cell redox homeostasis, cellular response to oxidative stress, and cytosol and nuclear localization
CAGL0L07656g	-1.24	-1.10	-1.17	-1.16	-1.13	-1.14	*GLO1*	Ortholog(s) have lactoylglutathione lyase activity, zinc ion-binding activity, role in glutathione metabolism and methylglyoxal catabolism to D-lactate, and cytosol and nuclear localization
CAGL0A04433g	-1.16	-1.16	-1.16	1.04	1.20	1.12	*PRX1*	Ortholog(s) have thioredoxin peroxidase activity, role in cell redox homeostasis, cellular response to oxidative stress, response to cadmium ions, and mitochondrial and nuclear localization
CAGL0A02530g	-1.08	-1.21	-1.14	1.02	1.20	1.11	*TRR1*	Thioredoxin reductase
CAGL0F00825g	-1.21	-1.09	-1.15	-1.25	-1.14	-1.19	*GSH2*	Ortholog(s) have glutathione synthase activity, role in cellular response to cadmium ions, glutathione biosynthetic process, phytochelatin biosynthetic process, and cytosol localization
CAGL0B03289g	-1.18	-1.02	-1.09	-1.04	-1.02	-1.03	*DUG2*	Ortholog(s) have gamma-glutamyltransferase activity, omega peptidase activity, role in glutathione catabolic process, and cytoplasm and nuclear localization
CAGL0F06017g	-1.03	-1.15	-1.09	1.13	1.07	1.10	*CCS1*	Putative copper chaperone for superoxide dismutase Sod1p
CAGL0I08503g	-1.03	-1.09	-1.06	-1.02	1.10	1.04	*MET16*	Ortholog(s) have phosphoadenylyl-sulfate reductase (thioredoxin) activity, role in cellular response to drugs, methionine biosynthetic process, and cytosol and nuclear localization

CAGL0M05643g	-1.01	-1.08	-1.04	-1.16	-1.03	-1.09	*YFH1*	Ortholog(s) have ferrous iron binding, ferroxidase activity, and iron chaperone activity, and roles in cellular iron ion homeostasis, cellular response to oxidative stress, glutathione metabolic process, and iron-sulfur cluster assembly
CAGL0I00264g	-1.00	-1.05	-1.02	1.15	1.17	1.16	*HYR1*	Has domain(s) with predicted glutathione peroxidase activity and roles in oxidation-reduction, response to oxidative stress; mass spectrometry data support an N-terminal extension of this ORF
CAGL0G04961g	-1.00	-1.00	-1.00	1.01	-1.04	-1.01	*GRX8*	Ortholog(s) have glutathione-disulfide reductase activity and cytoplasm localization
CAGL0G07271g	1.08	-1.25	-1.06	-1.01	1.24	1.12	*TSA1*	Putative thioredoxin peroxidase; protein differentially expressed in azole-resistant strain
CAGL0I00242g	1.01	-1.07	-1.03	1.02	1.09	1.06	- [c]	Has domain(s) with predicted glutathione peroxidase activity and roles in oxidation-reduction and response to oxidative stress
CAGL0I00924g	-1.05	1.01	-1.02	-1.10	1.04	-1.03	*GLO4*	Ortholog(s) have hydroxyacylglutathione hydrolase activity, roles in cellular carbohydrate metabolism, methylglyoxal catabolism to D-lactate, and localization in the cytosol, mitochondrial matrix, and nucleus
CAGL0J03146g	1.14	-1.15	1.00	1.08	1.06	1.07	*RNR1*	Ortholog(s) have nucleotide binding, ribonucleoside-diphosphate reductase activity, and thioredoxin disulfide as acceptor activity
CAGL0L06402g	-1.03	1.05	1.01	1.20	1.08	1.14	*YCF1*	Ortholog(s) have bilirubin transmembrane transporter activity, glutathione S-conjugate-exporting ATPase activity, and phytochelatin transmembrane transporter activity

CAGL0I00506g	-1.01	1.04	1.02	1.24	1.29	1.26	*ECM38*	Ortholog(s) have gamma-glutamyltransferase activity, roles in cellular response to nitrogen starvation, glutathione catabolism, xenobiotic metabolism, and localization to the endoplasmic reticulum and vacuole
CAGL0D03432g	1.19	-1.08	1.06	-1.31	-1.03	-1.15	*RNR4*	Ortholog(s) have ribonucleoside-diphosphate reductase activity, thioredoxin disulfide as acceptor activity, and roles in the cofactor biosynthetic process and deoxyribonucleotide biosynthetic process
CAGL0G04213g	1.21	-1.04	1.09	-1.06	-1.10	-1.08	*RNR2*	Ortholog(s) have ribonucleoside-diphosphate reductase activity, thioredoxin disulfide as acceptor activity, and roles in the deoxyribonucleotide biosynthetic process and nuclear and ribonucleoside-diphosphate reductase complex localization
CAGL0J05324g	1.03	1.06	1.04	1.19	1.31	1.25	*YJL068C*	Ortholog(s) have S-formylglutathione hydrolase activity and roles in the formaldehyde catabolic process and cytosol localization
CAGL0K06259g	1.14	1.00	1.07	1.52	1.15	1.33	*TSA2*	Thiol-specific antioxidant protein; predicted thioredoxin peroxidase involved in oxidative stress response; protein abundance decreased in ace2 mutant cells
CAGL0K00803g	1.08	1.26	1.17	1.34	1.54	1.44	*TRX1*	Protein described as thioredoxin involved in oxidative stress response; expression upregulated in biofilm vs. planktonic cell culture
CAGL0L01111g	1.11	1.45	1.28	-1.07	1.15	1.04	*SFA1*	Ortholog(s) have S-(hydroxymethyl)glutathione dehydrogenase activity, alcohol dehydrogenase (NAD) activity, and hydroxymethylfurfural reductase (NADH) activity

CAGL0C02035g	1.43	1.18	1.30	1.37	1.15	1.26	*DUG1*	Ortholog(s) have metallodipeptidase activity; omega peptidase activity; and roles in the glutathione catabolic process and cytosol, mitochondrial, nuclear, and ribosomal localization
CAGL0C04741g	1.14	1.63	1.39	1.47	1.88	1.68	*SOD1*	Cytosolic copper-zinc superoxide dismutase
CAGL0I01166g	1.94	1.30	1.62	2.18	1.76	1.97	*TRR2*	Thioredoxin reductase (NADPH)

[a] "Sc" stand for *Saccharomyces cerevisiae*.

[b] Description was obtained from Saccharomyces Genome Database (SGD)

[c] The ORF of CAGL0I00242g is uncharacterized, however has domain(s) with predicted glutathione peroxidase activity.

Figure Legends

Fig. 1. Oxidative stress response of *Candida glabrata* wild-type, Δ*vph2* mutant, and reconstituted strains

A. The logarithmic-phase cells grown with agitation in SC broth at 30°C were adjusted to 2 × 10^7 cells/ml, and then, 5 μl of serial 10-fold dilutions were spotted onto SC plates containing H_2O_2, diamide, or menadione at the indicated concentrations. Plates were photographed after 72 h of incubation at 30°C. B. Logarithmic-phase cells shaken at 30°C in SC broth (pH 5.0 or 7.2) (4 × 10^7 cells/ml) were incubated with 10 μM H_2DCFDA at 30°C for 15 min, and fluorescence was measured at a fluorescence excitation of 485 nm and emission at 530 nm. Fluorescence measurements were repeated three times on independent occasions. C. The growth was measured in shaking cultures at 30°C in SC broth (pH 5.0 or 7.2). ■: WT, ◆: Δ*vph2*, ▲: Δ*vph2*+*VPH2*. D. The growth was measured in shaking cultures at 30°C in SC broth (pH 7.2) and SC/MOPS broth (pH 7.2). ■: WT, ◆: Δ*vph2*, ▲: Δ*vph2*+*VPH2*. The growth curve was determined by cell count.

Fig. 2. Effects of NAC and DEM on intracellular ROS level and growth of *C. glabrata* wild-type, Δ*vph2* mutant, and reconstituted strains

A. Logarithmic-phase cells shaken at 30°C in SC broth (pH 5.0 or 7.2) in the presence and absence of 5 mM NAC (4×10^7 cells/ml) were incubated with 10 μM H_2DCFDA at 30°C for 15 min, and fluorescence was measured at a fluorescence excitation of 485 nm and emission at 530 nm. Fluorescence measurements were repeated three times on independent occasions. B. The growth was measured in shaking cultures at 30°C in SC broth (pH 5.0 or 7.2) in the presence and absence of 1 or 5 mM NAC. (■: 0 mM NAC, ◆: 1 mM NAC, ▲: 5 mM NAC) C. The growth was measured in shaking cultures at 30°C in SC broth (pH 5.0 or 7.2) in the presence and absence of 0.5 mM DEM. (■: 0 mM DEM, ◆: 0.5 mM DEM)

Fig. 3. Oxidative stress response of *C. glabrata* wild-type *rho*^{0} petite mutant and Δ*vph2* *rho*^{0} petite mutant strains

A. Logarithmic-phase cells shaken at 30°C in SC broth (pH 5.0 or 7.2) (4×10^7 cells/ml) were incubated with 10 μM H_2DCFDA at 30°C for 15 min, and fluorescence was measured at a fluorescence excitation of 485 nm and emission at 530 nm. Fluorescence measurements were repeated three times on independent occasions. B. The growth was measured in shaking cultures at 30°C in SC broth (pH 5.0 or 7.2). ■: wild-type, ◆: wild-type *rho*^{0} *petite* mutant 1, ▲: wild-type *rho*^{0} *petite* mutant 2, ●: Δ*vph2*, ○: Δ*vph2 rho*^{0} petite mutant 1, ×:

35 Δ*vph2 rho*^{0} petite mutant 2.

36

37 Fig. 4. Expression and enzyme activity of genes encoding antioxidant molecules and
38 enzymes
39 A. Total RNAs were extracted from logarithmic-phase cells shaken at 30°C in SC broth
40 (pH 5.0 or 7.2). Quantitative real-time PCR was performed as described in Experimental
41 Procedures. Expression levels of target genes were normalized to 18S rRNA. Results are
42 presented as fold expression relative to the levels in the wild-type grown in SC broth
43 (pH5.0). The PCR assays were repeated three times on independent occasions. B. Sample
44 solution was extracted from logarithmic-phase cells shaken at 30°C in SC broth (pH 5.0 or
45 7.2). Total SOD activity was measured using an SOD Assay Kit-WST. Mn-SOD activity
46 was measured by adding potassium cyanide (final concentration: 1 mmol/l) to the sample
47 solution. Catalase activity was measured using a catalase activity assay kit. Glutathione
48 quantification was measured using a GSSG/GSH quantification kit. These assays were
49 repeated three times on independent occasions.

50

51 Fig. 5. Oxidative stress response of *C. glabrata CTA1* and *SOD2*-overexpressed strains of

52 the wild-type and Δ*vph2* mutant

53 A. Total RNAs were extracted from logarithmic-phase cells shaken at 30°C in SC broth.
54 Quantitative real-time PCR was performed as described in Experimental Procedures.
55 Expression levels of *CTA1* and *SOD2* were normalized to 18S rRNA. Results are presented
56 as fold expression relative to the levels in the wild-type + pCgACT-P. The PCR assays
57 were repeated three times on independent occasions. B. Logarithmic-phase cells shaken at
58 30°C in SC broth (pH 5.0 or 7.2) (4×10^7 cells/ml) were incubated with 10 μM H_2DCFDA
59 at 30°C for 15 min, and fluorescence was measured at a fluorescence excitation of 485 nm
60 and emission at 530 nm. Fluorescence measurements were repeated three times on
61 independent occasions. C. *C. glabrata* cells were incubated with agitation in SC broth (pH
62 5.0 or 7.2) at 30°C and growth was monitored. ■: wild-type + pCgACT-P, ◆: wild-type +
63 *CTA1*-OE, ▲: wild-type + *SOD2*-OE, △: Δ*vph2* mutant + pCgACT-P, ○: Δ*vph2* mutant +
64 *CTA1*-OE, ●: Δ*vph2* mutant + *SOD2*-OE. D. The logarithmic-phase cells shaken at 30°C in
65 SC broth were adjusted to 2×10^7 cells/ml of SC broth, and then, 5 μl of serial 10-fold
66 dilutions were spotted onto SC plates containing H_2O_2, diamide, or menadione at the
67 indicated concentrations. Plates were photographed after 72 h of incubation at 30°C.

68

69 Fig. 6. Oxidative stress response of *C. glabrata* Δ*cta1*, Δ*sod2*, and Δ*cta1*Δ*sod2* double
70 mutant strains
71 A. Logarithmic-phase cells shaken at 30°C in SC broth (pH 5.0 or 7.2) (4×10^7 cells/ml)
72 were incubated with 10 μM H_2DCFDA at 30°C for 15 min, and fluorescence was measured
73 in shaking cultures at a fluorescence excitation of 485 nm and emission at 530 nm. B. The
74 growth was measured at 30°C in SC broth (pH 5.0 or 7.2). ■: wild-type, ×: Δ*vph2*, ▲:
75 Δ*cta1*, ◆: Δ*cta1*+*CTA1*, △: Δ*sod2*, ●: Δ*sod2*+*SOD2*, ○: Δ*cta1*Δ*sod2*. C. The
76 logarithmic-phase cells shaken at 30°C in SC broth were adjusted to 2×10^7 cells/ml of SC
77 broth, and then 5 μl of serial 10-fold dilutions were spotted onto SC plates containing H_2O_2,
78 diamide, or menadione at the indicated concentrations. Plates were photographed after 72 h
79 of incubation at 30°C.
80
81 Fig. 7. Effect of copper and iron on the OSR of *C. glabrata* wild-type and Δ*vph2* mutant
82 strains
83 A. Total RNAs were extracted from logarithmic-phase cells shaken at 30°C in SC broth
84 containing 0.1 mM copper or iron. Quantitative real-time PCR (qRT-PCR) was performed
85 as described in Experimental Procedures. Results are presented as fold expression relative

to the levels in the wild-type. The qRT-PCR assays were repeated three times on independent occasions. B. The cells shaken at 30°C in SC broth (pH 7.2) in the presence and absence of 0.1 mM copper or iron (4×10^7 cells/ml) were incubated with 10 μM H_2DCFDA at 30°C for 15 min, and fluorescence was measured at a fluorescence excitation of 485 nm and emission at 530 nm. C. The growth was measured in shaking cultures at 30°C in SC broth (pH 7.2) in the presence or absence of 0.1 mM copper or iron. ■: wild-type, ◆: wild-type with copper, ▲: wild-type with iron, △: Δ*vph2* mutant, ○: Δ*vph2* mutant with copper, ●: Δ*vph2* mutant with iron.

Fig. 8 The influence of V-ATPase on the OSR in *C. glabrata*

C. glabrata V-ATPase plays an important role in the regulation of *CTA1* and *SOD2* expression level, leading to proper response to endogenous and exogenous oxidative stress.

*1: The gene expression is dependent on the V-ATPase activity.

*2: We referred to the report by Zechmann *et al* (Zechmann 2011).

Figure 1.

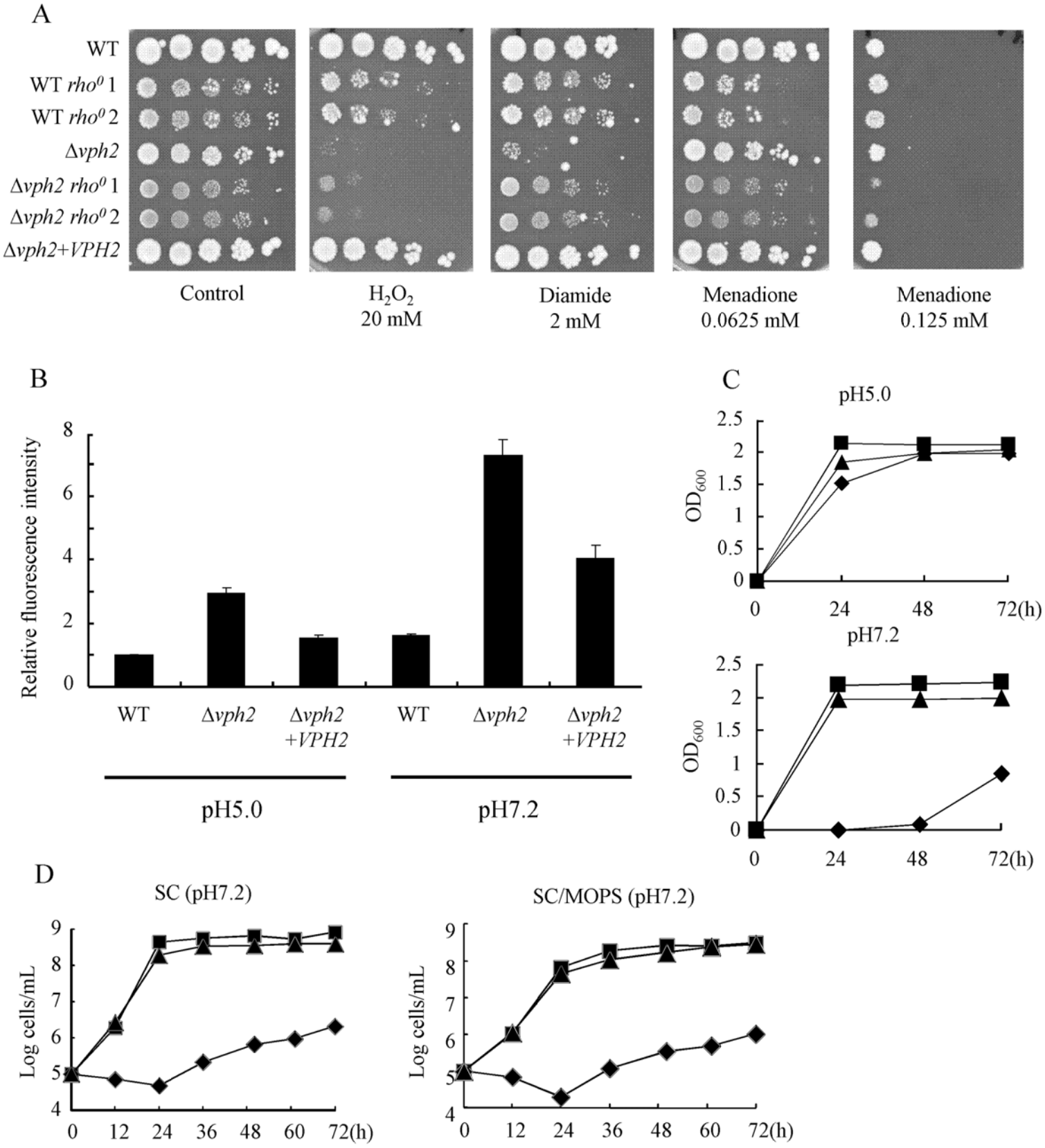
A
WT
WT rho0 1
WT rho0 2
Δvph2
Δvph2 rho0 1
Δvph2 rho0 2
Δvph2+VPH2
Control
H2O2 20 mM
Diamide 2 mM
Menadione 0.0625 mM
Menadione 0.125 mM
B
Relative fluorescence intensity
WT
Δvph2
Δvph2 +VPH2
pH5.0
pH7.2
C
pH5.0
pH7.2
OD600
72(h)
D
SC (pH7.2)
SC/MOPS (pH7.2)
Log cells/mL
72(h)

Figure 2.

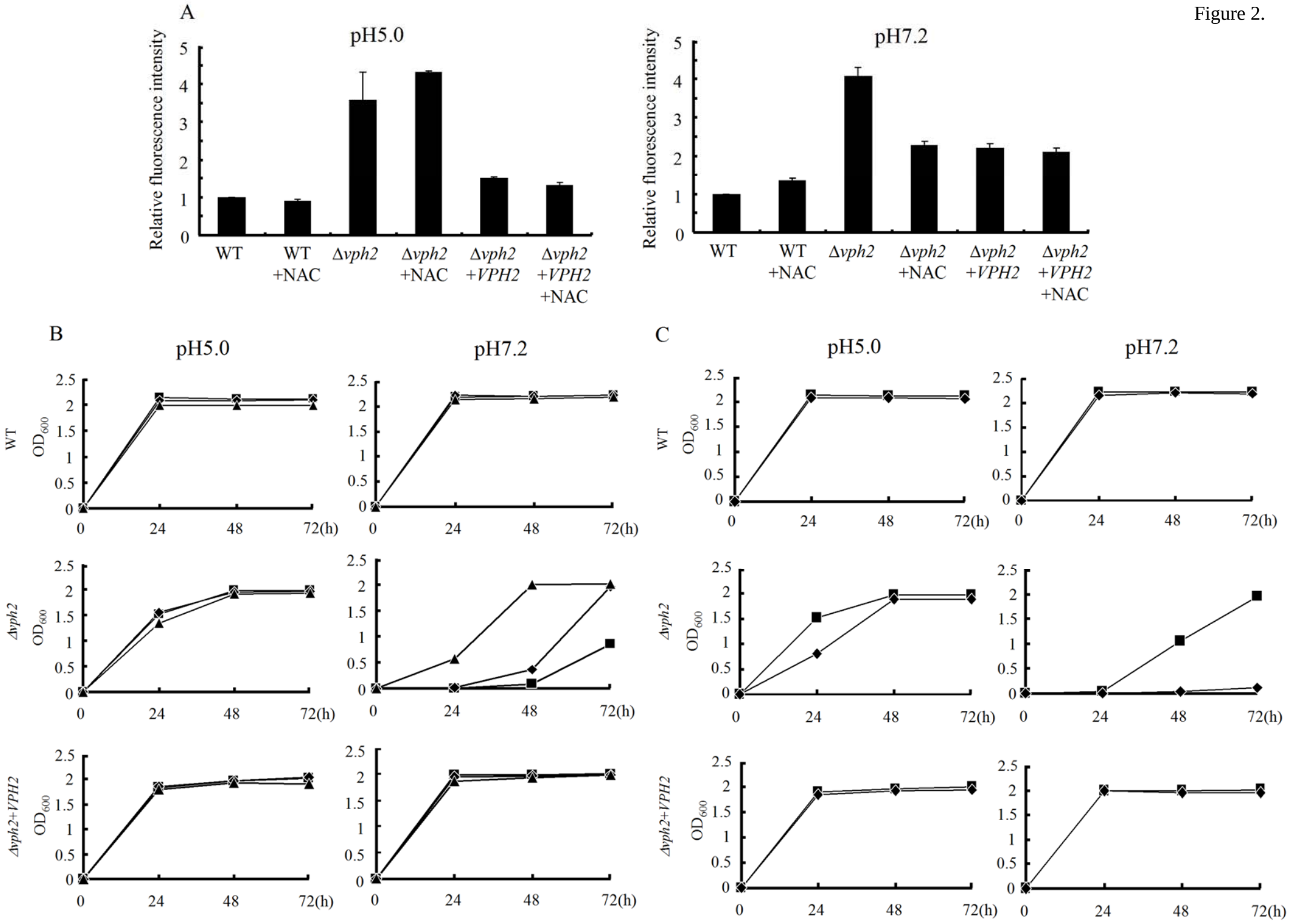
A
pH5.0
Relative fluorescence intensity
WT
WT +NAC
Δvph2
Δvph2 +NAC
Δvph2 +VPH2
Δvph2 +VPH2 +NAC
pH7.2
B
C
OD600
72(h)

Figure 3.

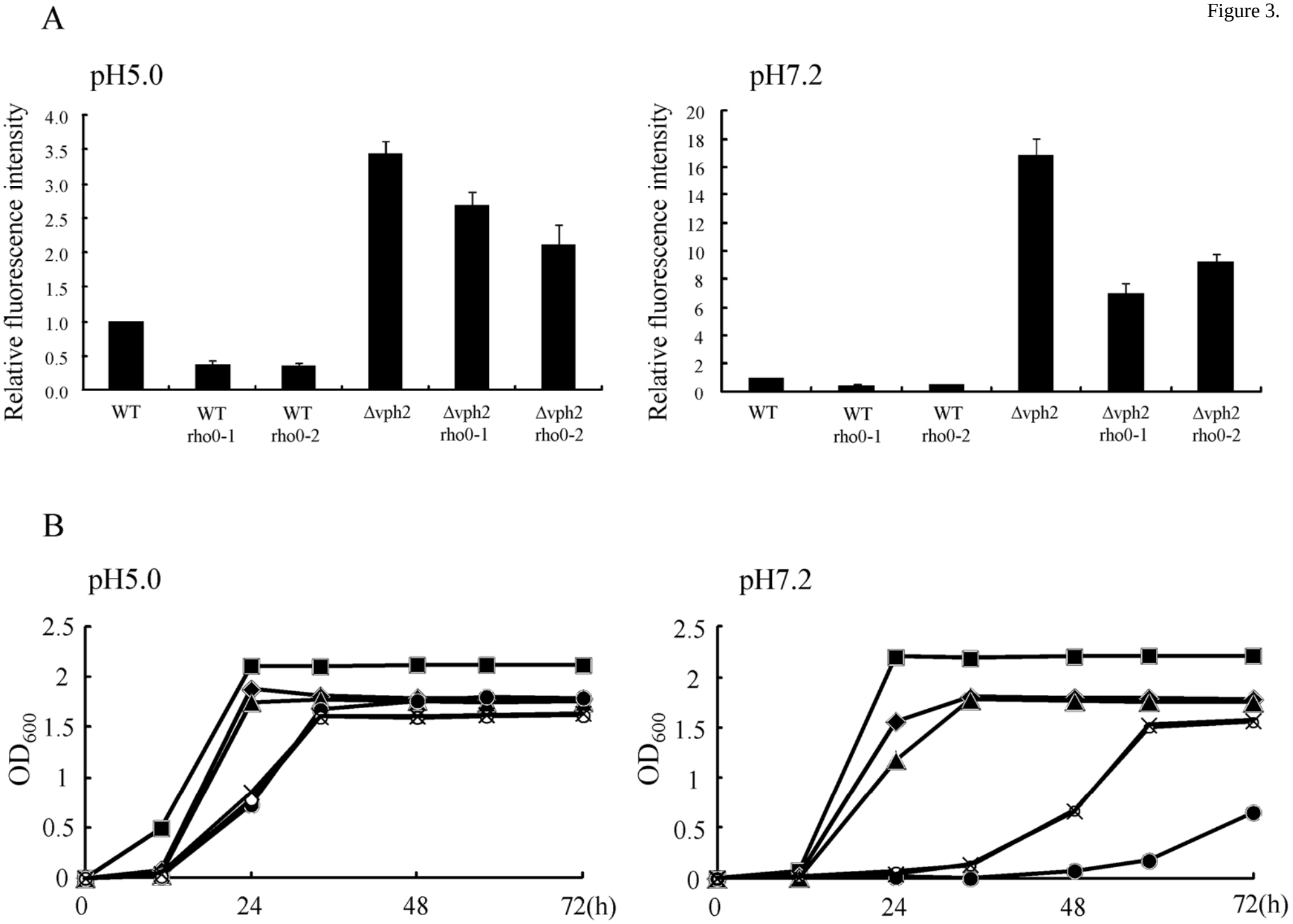
A
pH5.0
Relative fluorescence intensity
4.0
3.5
3.0
2.5
2.0
1.5
1.0
0.5
0.0
WT
WT rho0-1
WT rho0-2
Δvph2
Δvph2 rho0-1
Δvph2 rho0-2
pH7.2
Relative fluorescence intensity
20
18
16
14
12
10
8
6
4
2
0
WT
WT rho0-1
WT rho0-2
Δvph2
Δvph2 rho0-1
Δvph2 rho0-2
B
pH5.0
OD600
2.5
2
1.5
1
0.5
0
0
24
48
72(h)
pH7.2
OD600
2.5
2
1.5
1
0.5
0
0
24
48
72(h)

Figure 4.

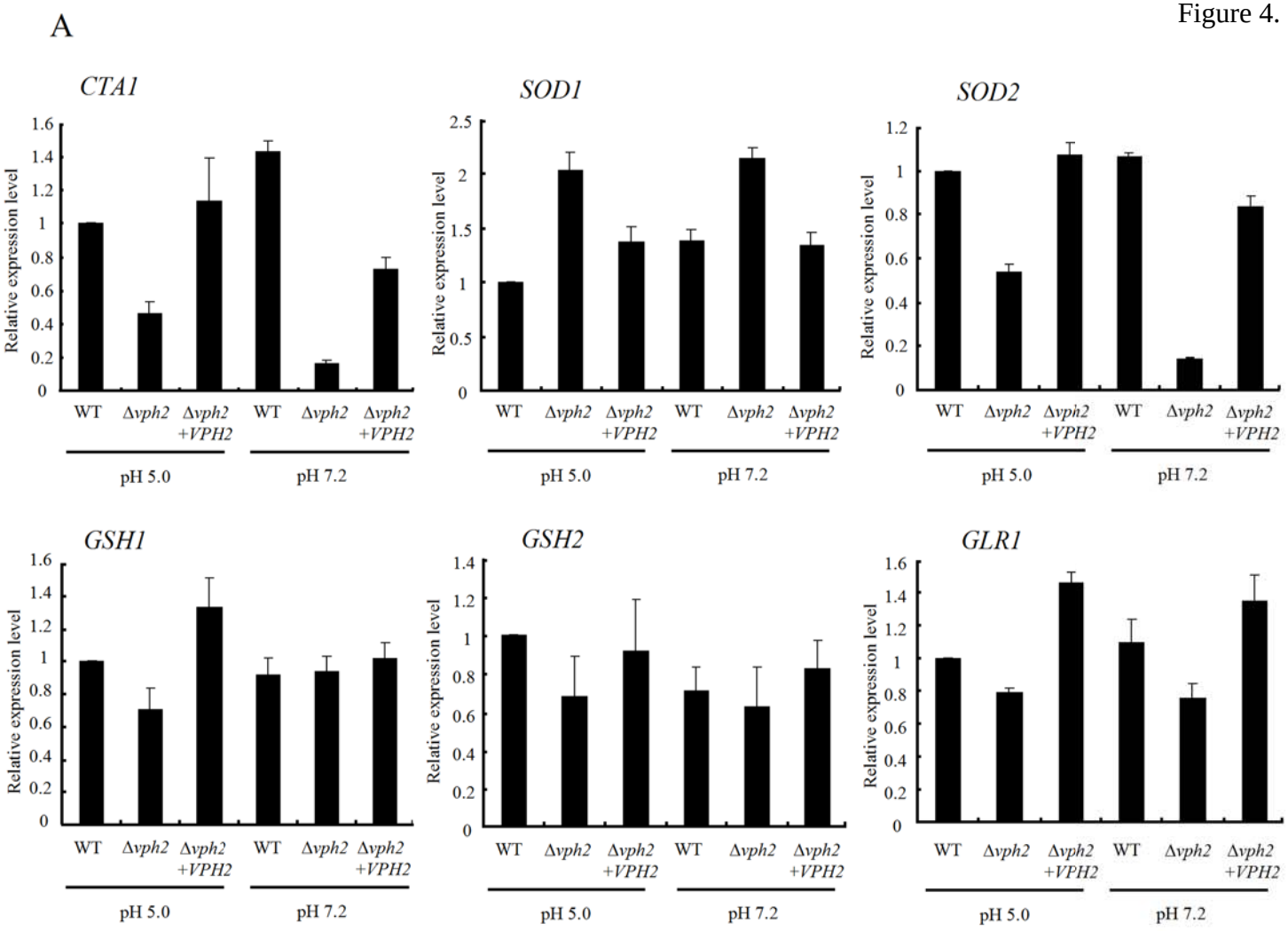
A
CTA1
SOD1
SOD2
GSH1
GSH2
GLR1
Relative expression level
WT
Δvph2
Δvph2 +VPH2
pH 5.0
pH 7.2

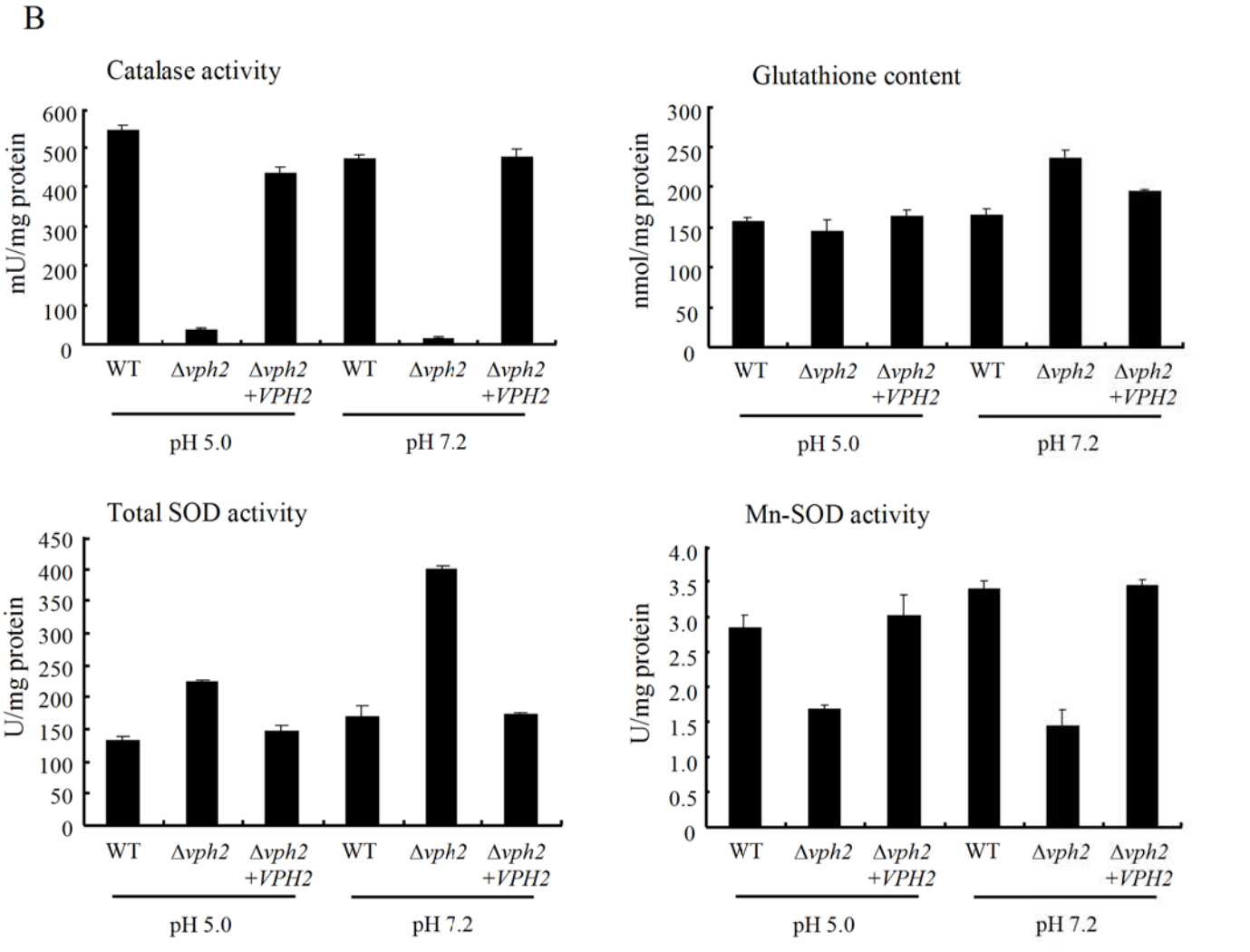
B
Catalase activity
mU/mg protein
Glutathione content
nmol/mg protein
Total SOD activity
U/mg protein
Mn-SOD activity
U/mg protein
WT
Δvph2
Δvph2 +VPH2
pH 5.0
pH 7.2

Figure 5.

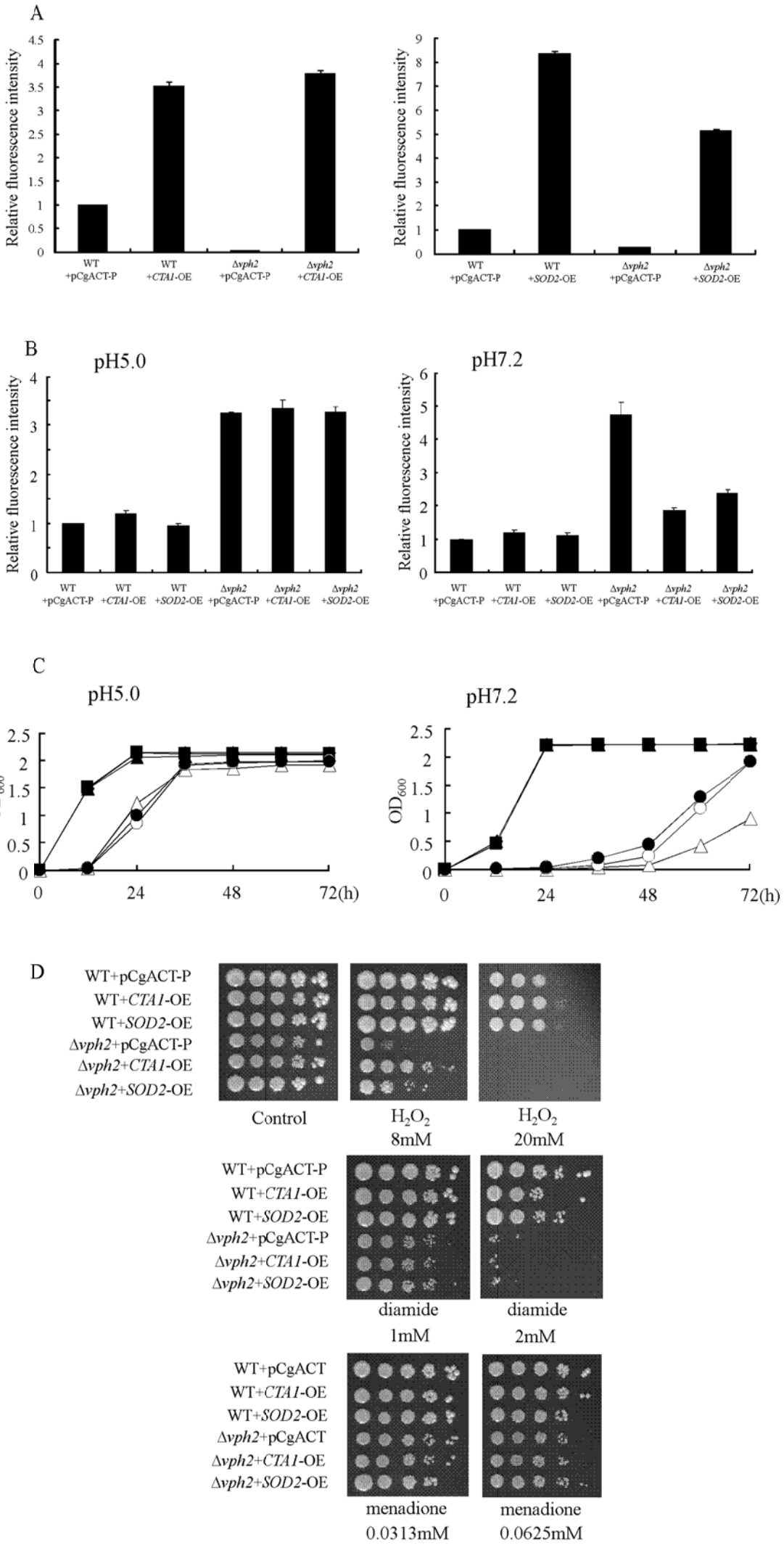
A
Relative fluorescence intensity
WT +pCgACT-P
WT +CTA1-OE
Δvph2 +pCgACT-P
Δvph2 +CTA1-OE
WT +SOD2-OE
Δvph2 +SOD2-OE
B
pH5.0
pH7.2
C
OD600
0
24
48
72(h)
D
WT+pCgACT-P
WT+CTA1-OE
WT+SOD2-OE
Δvph2+pCgACT-P
Δvph2+CTA1-OE
Δvph2+SOD2-OE
Control
H2O2 8mM
H2O2 20mM
diamide 1mM
diamide 2mM
WT+pCgACT
menadione 0.0313mM
menadione 0.0625mM

Figure 6.

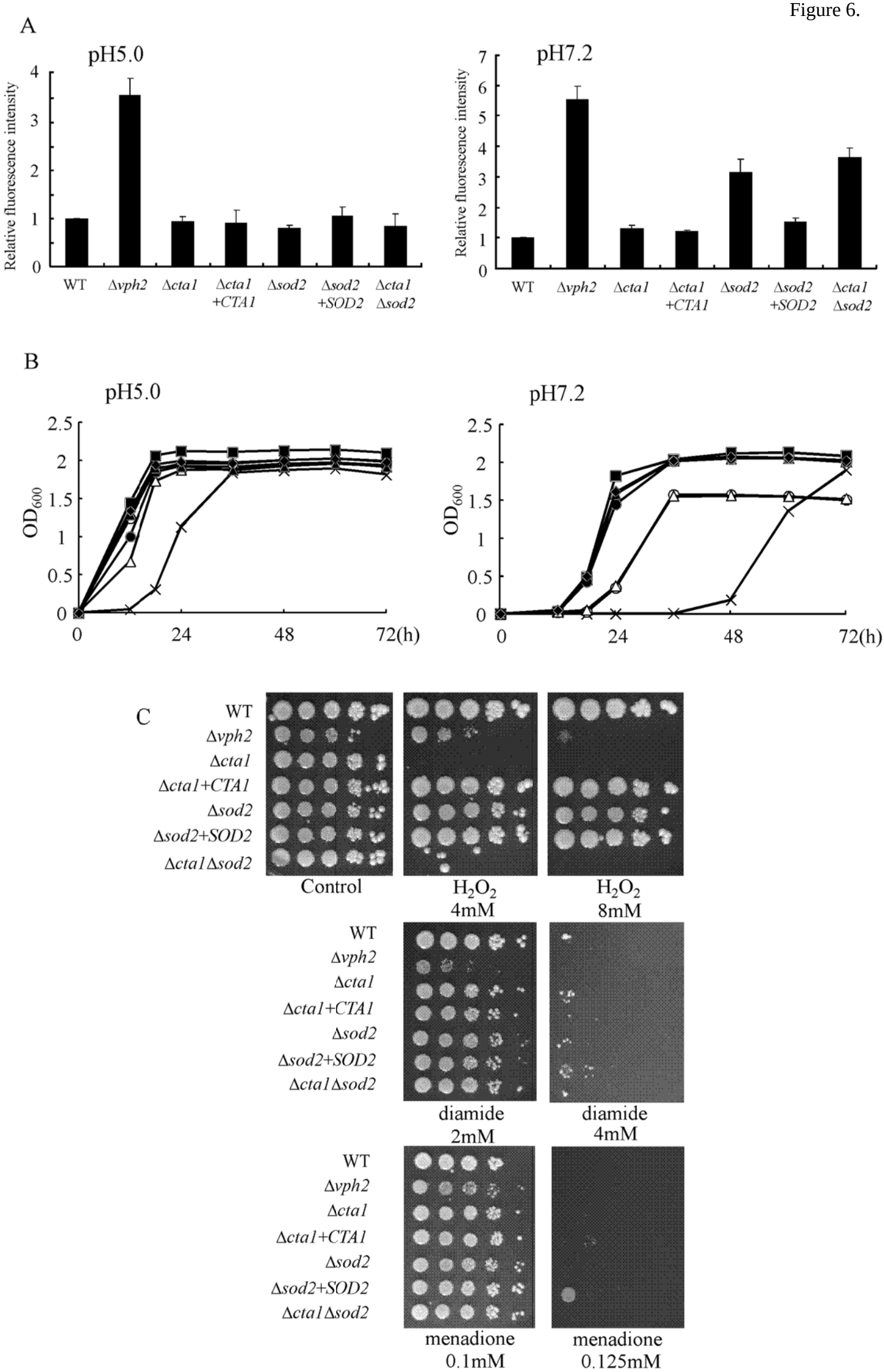
A
pH5.0
Relative fluorescence intensity
WT
Δvph2
Δcta1
Δcta1 +CTA1
Δsod2
Δsod2 +SOD2
Δcta1 Δsod2
pH7.2
B
pH5.0
pH7.2
OD600
0
24
48
72(h)
C
WT
Δvph2
Δcta1
Δcta1+CTA1
Δsod2
Δsod2+SOD2
Δcta1Δsod2
Control
H2O2 4mM
H2O2 8mM
diamide 2mM
diamide 4mM
menadione 0.1mM
menadione 0.125mM

Figure 7.

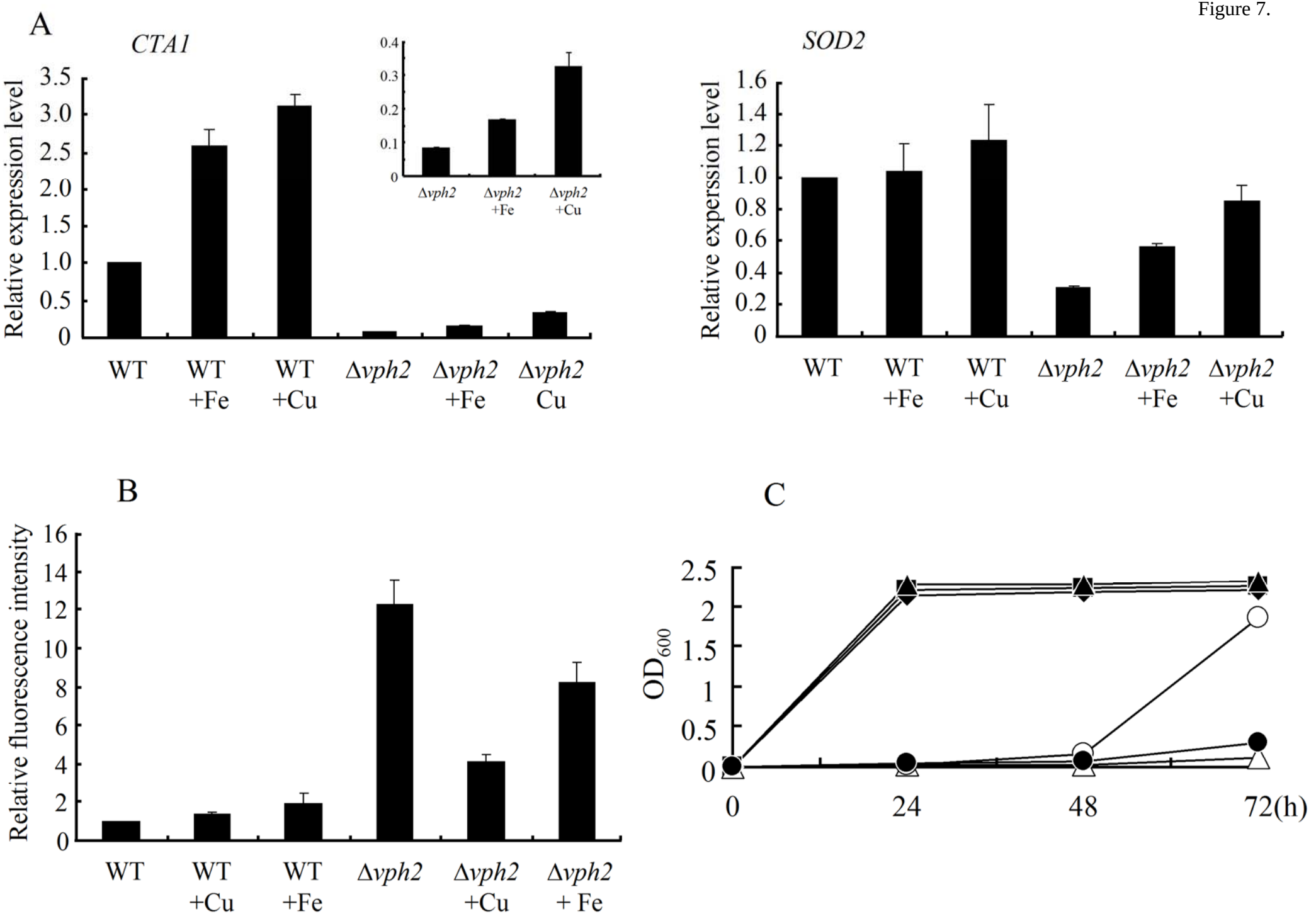
A
CTA1
Relative expression level
3.5
3.0
2.5
2.0
1.5
1.0
0.5
0
0.4
0.3
0.2
0.1
0
Δvph2
Δvph2 +Fe
Δvph2 +Cu
WT
WT +Fe
WT +Cu
Δvph2
Δvph2 +Fe
Δvph2 Cu
SOD2
Relative expression level
1.6
1.4
1.2
1.0
0.8
0.6
0.4
0.2
0
WT
WT +Fe
WT +Cu
Δvph2
Δvph2 +Fe
Δvph2 +Cu
B
Relative fluorescence intensity
16
14
12
10
8
6
4
2
0
WT
WT +Cu
WT +Fe
Δvph2
Δvph2 +Cu
Δvph2 + Fe
C
OD600
2.5
2
1.5
1
0.5
0
0
24
48
72(h)

Figure 8.

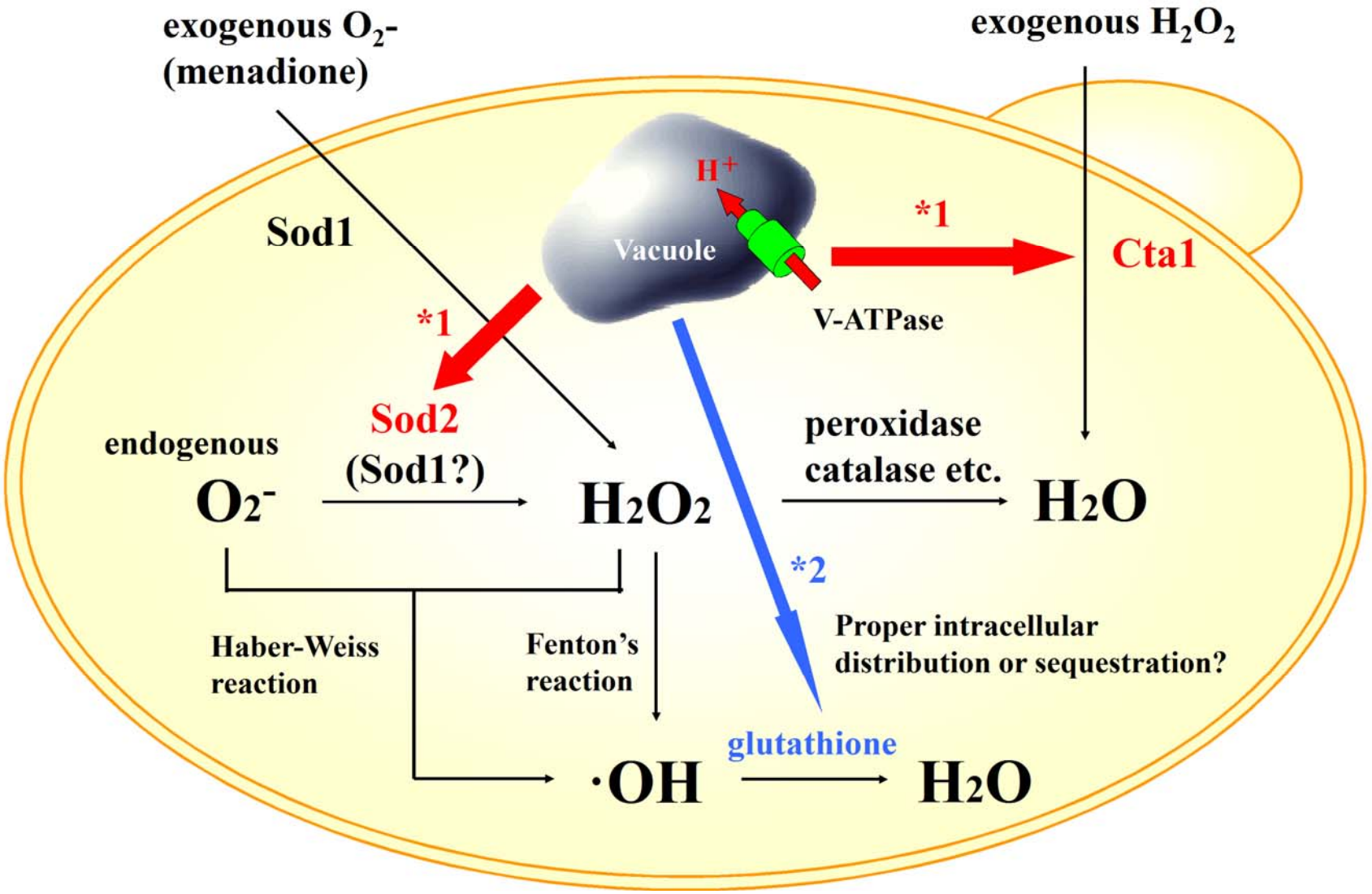
exogenous O_2-
(menadione)
exogenous H_2O_2
Sod1
Vacuole
H^+
*1
Cta1
V-ATPase
*1
Sod2
(Sod1?)
endogenous
O_2^-
H_2O_2
peroxidase
catalase etc.
H_2O
*2
Haber-Weiss
reaction
Fenton's
reaction
Proper intracellular
distribution or sequestration?
glutathione
·OH
H_2O